Sensitivity of tropospheric ozone to halogen chemistry in the chemistry-climate model LMDZ-INCA vNMHC

Cyril Caram[1], Sophie Szopa[1], Anne Cozic[1], Slimane Bekki[2], Carlos A. Cuevas[3] and Alfonso Saiz-Lopez[3]

[1]Laboratoire des Sciences du Climat et de l'Environnement, LSCE/IPSL, CEA-CNRS-UVSQ, Université Paris-Saclay, Gif-sur-Yvette, France
[2]Laboratoire Atmosphère, Milieux, Observations Spatiales, Institut Pierre Simon Laplace, LATMOS/IPSL, CNRS-UVSQ-Sorbonne Université, Guyancourt and Paris, France
[3]Department of Atmospheric Chemistry and Climate, Institute of Physical Chemistry Rocasolano, CSIC, Madrid, Spain

Correspondence to: Sophie Szopa (sophie.szopa@lsce.ipsl.fr)

Abstract. The atmospheric chemistry of halogenated species (Cl, Br, I) participates in the global chemical sink of tropospheric ozone and perturbs the oxidizing capacity of the troposphere, notably by influencing the atmospheric lifetime of methane. Global chemistry-climate models are commonly used to assess the global budget of ozone, its sensitivity to emissions of its precursors, and to project its long-term evolution. Here, we report on the implementation of tropospheric sources and chemistry of halogens in the chemistry-climate model LMDZ-INCA and its effects on the tropospheric ozone budget. Overall, the results show that the model simulates satisfactorily the impact of halogens on the photooxidizing system in the troposphere, in particular in the marine boundary layer. To quantify the effects of halogen chemistry in LMDZ-INCA, standard metrics representative of the behavior of the tropospheric chemical system (O_x, HO_x, NO_x, CH_4, and NMVOCs) are computed with and without halogens. Addition of tropospheric halogens in the LMDZ-INCA model leads to a decrease of 22% in the ozone burden, 8% in OH, and 33% in NOx. Sensitivity simulations show for the first time that the inclusion of halogen chemistry makes ozone more sensitive to perturbations in CH_4, NO_x, and NMVOCs. Consistent with other global model studies, the sensitivity of the tropospheric ozone burden to changes from pre-industrial to present-day emissions is found to be ~20% lower when tropospheric halogens are taken into account.

1 Introduction

If the atmospheric chemistry of halogenated species was first studied for its importance for the composition of the stratosphere and in particular the ozone layer (Molina and Rowland, 1974; Stolarski and Cicerone, 1974), its importance for tropospheric chemistry was also suggested as soon as the early 1980s (Chameides and Davis, 1980). With the progress of measurement techniques, marine aerosols were thought to harbor and release reactive halogens into the gas-phase (Cicerone, 1981). Later on, halogenated species were found to be responsible for ozone destruction in the Arctic troposphere (Bottenheim et al., 1990; Oltmans and Komhyr, 1986). Meanwhile, natural and anthropogenic sources of halogens were starting to be identified and characterized (Graedel and Keene, 1995; Lobert et al., 1999; McCulloch et al., 1999; Carpenter, 2003; Platt and Hönninger, 2003; Saiz-Lopez and Plane, 2004). In recent years, the addition of halogenated chemistry into global chemistry-transport models have revealed their significant influence on the photo-oxidizing chemistry of the troposphere on a global scale (Saiz-Lopez et al., 2012a; Simpson et al., 2015). This influence arises from the high reactivity of atomic halogens (e.g., Cl, Br, I) and halogen oxides radicals (e.g., ClO, BrO, IO and higher oxides), which are produced in the atmosphere by the decomposition of very short-lived halogenated substances (VSLS), by heterogeneous reactions on sea salt aerosols, and, in the case of iodine, also released via ozone deposition to the ocean surface. They can also be generated by polar specific halogen activation mechanisms on sea ice surfaces, blowing snow and the snowpack (as reviewed by Abbatt et al. 2012).

Details on the tropospheric chemistry of chlorine, bromine and iodine can be found in review articles (e.g. Saiz-Lopez and von Glasow, 2012; Simpson et al., 2015). Reactive halogen species mainly affect tropospheric chemistry by (1) modifying the partitioning of HO_x (HO_2 + OH) and nitrogen oxides ($NO_x = NO_2 + NO$) and reacting with NO_2 to form species that remove NOx from the system via deposition or other loss processes; (2) being involved in the oxidation of non-methane volatile organic compounds (NMVOCs) and mercury; (3) participating in the formation of new particles (Giorgi and Chameides, 1985; O'Dowd et al., 2002; von Glasow et al., 2004; Gómez Martín et al., 2020; Saiz-lopez et al., 2012); and (4) constituting a sink for tropospheric ozone at the global scale. Halogenated species play a role in the ozone and hydroxyl radical (OH) budgets and therefore influence the oxidative capacity of the troposphere (Iglesias-Suarez et al., 2020). In addition, by influencing the abundances of tropospheric ozone, which is an important greenhouse gas, halogens can indirectly affect the climate (Saiz-Lopez et al., 2012b; Hossaini et al., 2015; Sherwen et al., 2017).

The loss of tropospheric ozone by halogens is mainly induced by iodine and bromine species with a lower contribution of chlorine species (Sherwen et al., 2016a). It can be caused by direct catalytic ozone destruction and reduction in ozone production through the removal of NO_2 by halogen radicals. Halogen chemistry is thought to be especially active in pristine atmospheres that host 60 to 70% of the global burden of tropospheric ozone (Holmes et al., 2013). Based on model calculations, the halogen-driven ozone loss is estimated to be around 30% in the marine boundary layer (von Glasow et al., 2002, 2004; Saiz-Lopez et al., 2014; Sherwen et al., 2016a) and 5% to 20% globally (Yang et al., 2005; Saiz-Lopez et al., 2012b, 2014; Sherwen et al., 2016a), going up to 25 to 30% in Badia et al., 2019. Consequently, it might be important to consider halogens in chemistry-climate modelling. It could also help to reconstruct more reliably past atmospheric compositions (Saiz-Lopez et al., 2014; Young et al., 2013).

Despite its potential importance, only three global chemistry models have so far implemented detailed representations of halogenated (Cl, Br and I) tropospheric chemistry: CAM-Chem (Saiz-Lopez et al. 2012), GEOS-Chem (Sherwen 2016a) and TOMCAT (Hossaini et al. 2015). Halogen chemistry is complex with a high computational cost, Earth System Models used to assess how the evolution of atmospheric composition influences climate need to find the right compromise between the level of details (e.g. number of species and processes) for halogen chemistry representations here and the computing efficiency (Box 6.1 in Szopa et al. 2021). Indeed, the computational cost has to be sufficiently low for multiple long chemistry-climate simulations. So far, none of the chemistry-climate models involved in recent large intercomparison projects included tropospheric chemistry of very short-lived halogens and hence the impacts of their chemistry on key short-lived climate forcers (such as ozone and methane). Such multi-model projects are important. They are used to assess the budget of key chemical species, which can impact directly or indirectly climate or global air quality, and their sensitivity to changes in anthropogenic and natural emissions. The results are also used to evaluate the effects of international policies (e.g. Protocol to Abate Acidification, Eutrophication and Ground-level Ozone called Gothenburg Protocol) by quantifying source-receptor relations at continental scales (in the case of Hemispheric Transport of Air Pollution project, HTAP, Fiore et al., 2009), to explore the sensitivity of short lived climate forcers to changes in emissions of their precursors since the preindustrial period, or to project their possible future evolutions under a range of scenario assumptions (in the case of Atmospheric Chemistry and Climate Model Intercomparison Project (ACCMIP, Young et al., 2013) or, more recently, the Aerosol Chemistry Model Intercomparison Project (AerChemMIP, Stevenson et al., 2020).

The primary purpose of this work is to assess whether iodine, bromine and chlorine chemistry can, beyond their already established effect on global tropospheric ozone budget, affect the sensitivity of ozone to the changes of its precursors. In order to do so, we implemented a simplified representation of tropospheric halogen chemistry in a global chemistry-climate model, the LMDZ-INCA model (Laboratoire de Météorologie Dynamique (LMD) General Circulation Model, LMDZ; Interactions with Chemistry and Aerosols, INCA) with a focus on reproducing the overall effect of halogen chemistry on global tropospheric ozone. Results of the 3 global tropospheric chemistry models that already include detailed representations of this chemistry are used to guide the choices of the chemical reactions and emissions in our simple halogen scheme, and to assess

the LMDZ-INCA simulations. First, we evaluate the ability of the model to simulate the global tropospheric budget of halogens and their effect on ozone and by using the results of the CAM-Chem and GEOS-Chem models as references. The limitations of our model are also discussed, notably how some simplifications in our model affect the simulation of the spatial distribution of some specific halogenated species. Second, we investigate how the sensitivities of ozone, methane and hydroxyl radical to perturbations in anthropogenic emissions of photooxidant precursors change when halogen chemistry is accounted for. For instance, we explore changes in ozone burden and net destruction in simulations considering present-day (PD) and pre-industrial (PI) emissions with and without halogen chemistry. Finally, the last section recalls key findings and we conclude with implications for chemistry-climate simulations of tropospheric ozone evolution.

2 Methodology

2.1 Model description

2.1.1 LMDZ-INCA

LMDZ is an atmospheric general circulation model developed by Sadourny and Laval (1984). The primitive equations of the GCM are solved with a time step of 3 minutes, a large-scale transport of tracers is carried out every 15 minutes and the physical processes are calculated at a time interval of 30 minutes. The LMDZ model provides at each time step the physical quantities (temperature, pressure, water vapor, turbulence, boundary layer, etc.) needed to compute the transport and chemistry in INCA.

INCA is an atmospheric chemistry model developed at LSCE (Laboratoire des Sciences du Climat et de l'Environnement). The model takes into account the primary emissions from natural sources or by anthropogenic activities. It computes physical processes such as dry and wet deposition and photochemical reactions (Hauglustaine et al., 2004). The atmospheric concentration fields are integrated in time by solving differential equations when called by LMDZ, with a time step of 30 minutes. For this development, we used a version of INCA (version v_5.2.1) simulating interactively the gaseous photochemistry whereas aerosols distribution obtained with a more complex version of INCA are prescribed through climatologies. This version represents in particular the chemistry of the inorganic species O_x, NO_x and HO_x as well as CH_4, CO, non-methane volatile organic compounds (NMVOCs) and their photooxidized products (Folberth et al., 2006).

Biogenic emissions like those of isoprene are provided by the global vegetation model, ORCHIDEE (Organising Carbon and Hydrology In Dynamic Ecosystems) (Folberth et al., 2006). Anthropogenic emissions are based on the CEDS v2016-07-2 emission inventory for the year 2010 (Hoesly et al., 2018).

The LMDZ-INCA model has been used and assessed in numerous previous model intercomparison exercises aimed at simulating the preindustrial, present and future tropospheric composition (e.g. Szopa et al., 2013), the Hemispheric Transport of Air Pollution (HTAP) or chemistry/climate interactions such as ACCMIP (Naik et al., 2013).

2.1.2 Halogen chemistry

The chemistry of halogenated compounds implemented in LMDZ-INCA is essentially based on the scheme developed for CAM-Chem (Fernandez et al., 2014b; Ordóñez et al., 2012; Prados-Roman et al., 2015a; Saiz-Lopez et al., 2012b, 2014, 2015) and GEOS-Chem (Sherwen et al. 2016b), with a priority given to the reactions of importance for the ozone sinks (Figure 1).
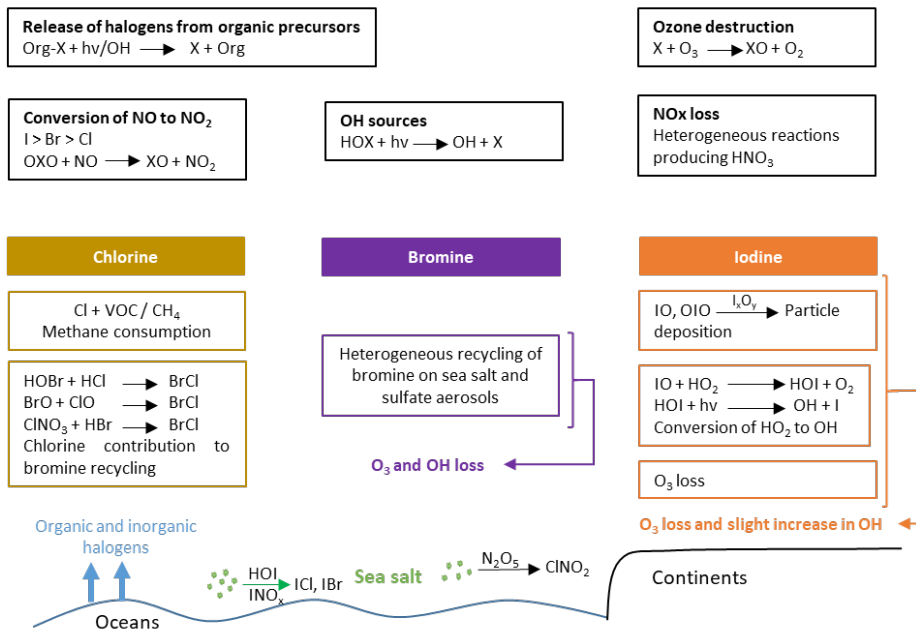
Figure 1: Schematic of the most important tropospheric chemical processes involving halogenated compounds (containing Cl, Br, I) as represented in LMDZ-INCA.

A total of 42 halogenated species have been added to the INCA chemical scheme (Table 1). The list of the 160 chemical
120 reactions added to the INCA chemical scheme can be found in Tables 2, 3, 4 and 5. Photolysis reactions of halogens as well
as relative quantum yields and absorption cross-sections are listed in Table 2. Uptake coefficients for heterogeneous reactions
are based on experimental values and data used by modellers and are reported in Table 5. Recycling through heterogeneous
chemistry on sea salt and sulfate aerosols is included while the heterogeneous bromine reactions in water droplets and on ice
crystals in clouds are not. Dry deposition is calculated with the Wesely scheme (Wesely, 1989) while washout of gases by
125 precipitation is simulated by using Henry's law constants detailed in Table S1 (Supplementary Material).

| a supprimé: literature |

| a supprimé: values |

| a supprimé: (Jacob, 2000; Sander et al., 2006; Ordóñez et al., 2012) |

Table 1. List of halogen tracers in INCA.

Tracer	Name	Processes affecting the tracer				
		chemistry	advection/convection	emissions [a]	Dry deposition	Wet deposition
Br_2	Dibromine	●	●	-	●	●
Br	Bromine	●	-	-	-	-
BrO	Bromine monoxide	●	-	-	-	-
$HOBr$	Hypobromous acid	●	●	-	●	●
HBr	Hydrogen bromide	●	●	-	●	●
$BrNO_2$	Bromine nitrite	●	●	-	●	●
$BrNO_3$	Bromine nitrate	●	●	-	●	●
CH_3Br	Bromomethane	●	●	●	-	-
CH_2Br_2	Dibromomethane	●	●	●	-	-
I_2	Diiodine	●	●	●	●	●

I	Iodine	●	-	-	-	-
IO	Iodine monoxide	●	-	-	-	-
OIO	Dioxidoiodine	●	-	-	-	-
HOI	Hypoiodous acid	●	●	●	●	●
HI	Hydrogen iodide	●	●	-	●	●
INO	Nitrosyl iodide	●	●	-	-	-
INO$_2$	Iodine nitrite	●	●	-	●	●
INO$_3$	Iodine nitrate	●	●	-	●	●
CH$_3$I	Iodomethane	●	●	●	-	-
CH$_2$I$_2$	Diiodomethane	●	●	●	-	-
I$_2$O$_2$	Iodooxy hypoiodite	●	●	-	●	●
I$_2$O$_3$	Iodo iodate	●	●	-	●	●
I$_2$O$_4$	Iodosyl iodate	●	●	-	●	●
I$_{aer}$	Aerosol iodine	-	●	-	●	●
Cl$_2$	Dichlorine	●	●	-	●	●
Cl	Chlorine	●	-	-	-	-
HCl	Hydrogen chloride	●	●	●	●	●
ClO	Chlorine monoxide	●	-	-	-	-
ClNO$_2$	Chlorine nitrite	●	●	■	●	●
ClNO$_3$	Chlorine nitrate	●	●	-	●	●
ClOO	Chlorine superoxide	●	-	-	-	-
OClO	Chlorine dioxide	●	-	-	-	-
HOCl	Hydrochlorous acid	●	●	-	●	●
Cl$_2$O$_2$	Dichlorine dioxide	●	●	-	-	-
CH$_3$Cl	Chloromethane	●	●	●	-	-
CH$_2$Cl$_2$	Dichloromethane	●	●	●	-	-
CHCl$_3$	Trichloromethane	●	●	●	-	-
CH$_2$IBr	Bromoiodomethane	●	●	●	●	-
CH$_2$ICl	Chloroiodomethane	●	●	●	●	-
IBr	Iodine monobromide	●	●	■	●	●
ICl	Iodine monochloride	●	●	■	●	●
BrCl	Bromine monochloride	●	●	-	●	●

[a] surface source ● or net chemical source from seasalts ■

135

Table 2. Photolysis reactions of halogens included in the scheme. * J$_{29}$ φ$_2$ (λ < 308 nm) = 0.6, φ$_2$ (λ=308-364 nm) = 7.143 x 10^{-3} λ (nm) – 1.60, φ$_2$(λ > 364 nm) = 1.0 and J$_{30}$, φ$_{30}$(λ) = 1- φ$_{29}$(λ).

Reaction	Quantum yield φ	Reference for absorption cross-section
$Br_2 + hv \rightarrow 2Br$	1	Sander et al. (2011)
$BrNO_2 + hv \rightarrow Br + NO_2$	1	Sander et al. (2011)
$BrONO_2 + hv \rightarrow BrO + NO_2$	0.15	Sander et al. (2011)
$BrONO_2 + hv \rightarrow Br + NO_2$	0.85	Sander et al. (2011)
$BrO + hv \rightarrow Br$	1	Sander et al. (2011)
$CH_3Br + hv \rightarrow Br$	1	Sander et al. (2011)
$CH_2Br_2 + hv \rightarrow 2Br$	1	Sander et al. (2011)
$CHBr_3 + hv \rightarrow 3Br$	1	Sander et al. (2011)
$HOBr + hv \rightarrow Br + OH$	1	Sander et al. (2011)
$BrCl + hv \rightarrow Br + Cl$	1	Sander et al. (2011)
$CH_2IBr + hv \rightarrow I + Br$	1	Sander et al. (2011)
$IBr + hv \rightarrow I + Br$	1	Sander et al. (2011)
$CH_2I_2 + hv \rightarrow 2I$	1	Sander et al. (2011)
$CH_3I + hv \rightarrow I$	1	Sander et al. (2011)
$HOI + hv \rightarrow I + OH$	1	Sander et al. (2011)
$INO_3 + hv \rightarrow I + NO_3$	1	Sander et al. (2011)
$I_2 + hv \rightarrow 2I$	1	Sander et al. (2011)

INO$_2$ + hv → I + NO$_2$	1		Sander et al. (2011)
INO + hv → I +NO	1		Sander et al. (2011)
IO + hv → I	0.91		Sander et al. (2011)
OIO + hv → I + O$_2$	1		Sander et al. (2011)
ICl + hv → I +Cl	1		Sander et al. (2011)
CH$_2$ICl + hv → I +Cl	1		Sander et al. (2011)
CH$_2$Cl$_2$ + hv → 2Cl	1		Sander et al. (2011)
CH$_3$Cl + hv → Cl + CH$_3$O$_2$	1		Sander et al. (2011)
Cl$_2$O$_2$ + hv → Cl + ClOO	1		Sander et al. (2011)
Cl$_2$ + hv → 2Cl	1		Sander et al. (2011)
ClNO$_2$ + hv → Cl + NO$_2$	1		Sander et al. (2011)
ClONO$_2$ + hv → Cl + NO$_2$	*		Sander et al. (2011)
ClONO$_2$ + hv → ClO + NO$_2$	*		Sander et al. (2011)
ClOO + hv → ClO + O$_2$	1		Sander et al. (2011)
ClO + hv → Cl	1		Sander et al. (2011)
HOCl + hv → Cl + OH	1		Sander et al. (2011)
OClO + hv → ClO + O	1		Sander et al. (2011)
I$_2$O$_2$ + hv → I + OIO	0.21		Gómez Martin et al. (2005); Spietz et al. (2005)
I$_2$O$_3$ + hv → IO + OIO	0.21		Gómez Martin et al. (2005); Spietz et al. (2005)
I$_2$O$_4$ + hv → 2 OIO	0.21		Gómez Martin et al. (2005); Spietz et al. (2005)

140

Table 3. Bimolecular halogen reactions included in scheme. The scheme includes reations integrated in GEOS-Chem (Parrella et al., 2012; Eastham et al., 2014; Schmidt et al., 2016; Sherwen et al., 2016a; Sherwen et al., 2016b), TOMCAT (Hossaini et al., 2016) and Thomas et al., 2011. Species names are detailed in Folberth et al., 2006.

Reaction	A_0 (molécules^{-2}cm^{6}s^{-1})	-E_a/R (K)	Reference
Cl + CH$_3$O$_2$ → ClO + CH$_2$O + HO$_2$	1.60 x 10^{-10}		Sander et al. (2011)
Cl + CH$_3$OOH → HCl + CH$_3$O$_2$	5.70 x 10^{-11}		Sander et al. (2011)
Cl + C$_2$H$_6$ → HCl + C$_2$H$_5$O$_2$	7.20 x 10^{-11}	-70	Sander et al. (2011)
Cl + C$_2$H$_5$O$_2$ → ClO + HO$_2$ + CH$_3$CHO	7.40 x 10^{-11}		Sander et al. (2011)
Cl + C$_2$H$_5$OH → HCl + CH$_3$CHO	9.60 x 10^{-11}		Sander et al. (2011)
Cl + CH$_3$COOH → HCl + CH$_3$O$_2$ + CO$_2$	2.80 x 10^{-14}		Sander et al. (2011)
Cl + C$_3$H$_8$ → HCl + C$_3$H$_7$O$_2$	7.85 x 10^{-11}	-80	Sander et al. (2011)
Cl + C$_3$H$_8$ → HCl + PROPAO$_2$	6.54 x 10^{-11}		Sander et al. (2011)
Cl + CH$_3$COCH$_3$ → HCl + PROPAO$_2$	7.70 x 10^{-11}		Sander et al. (2011)
Cl + ISOP → HCl + ISOPO$_2$	7.70 x 10^{-11}	500	Sander et al. (2011)
Cl + CH$_3$OH → HCl + CH$_2$O + HO$_2$	5.50 x 10^{-11}		Sander et al. (2011)
Cl + ALKAN → HCl + ALKANO$_2$	2.05 x 10^{-10}		Atkinson et al. (2006)
Cl + C$_3$H$_6$ → HCl + PROPEO$_2$	3.60 x 10^{-12}		Atkinson et al. (2006)
Cl + CH$_3$Cl → CO + 2 HCl + HO$_2$	2.17 x 10^{-11}	-1130	Sander et al. (2011)
Cl + H$_2$O$_2$ → HCl + HO$_2$	1.10 x 10^{-11}	-980	Sander et al. (2011)
Cl + HO$_2$ → HCl + O$_2$	1.40 x 10^{-11}	270	Sander et al. (2011)
Cl + HO$_2$ → ClO + OH	3.60 x 10^{-11}	-375	Sander et al. (2011)
Cl + O$_3$ → ClO + O$_2$	2.30 x 10^{-11}	-200	Sander et al. (2011)
Cl + ClNO$_3$ → Cl$_2$ + NO$_3$	6.50 x 10^{-12}	135	Sander et al. (2011)
ClO + ClO → Cl$_2$ + O$_2$	1.00 x 10^{-12}	-1590	Sander et al. (2011)
ClO + ClO → OClO + Cl	3.50 x 10^{-13}	-1370	Sander et al. (2011)
ClO + ClO → Cl + ClOO	3.00 x 10^{-11}	-2450	Sander et al. (2011)
ClO + HO$_2$ → O$_2$ + HOCl	2.60 x 10^{-12}	290	Sander et al. (2011)
ClO + NO → Cl + NO$_2$	6.40 x 10^{-12}	290	Sander et al. (2011)
ClOO + Cl → 2 ClO	1.20 x 10^{-11}		Sander et al. (2011)
ClOO + Cl → Cl$_2$ + O$_2$	2.30 x 10^{-10}		Sander et al. (2011)
ClO + CH$_3$O$_2$ → ClOO + HO$_2$ + CH$_2$O	3.30 x 10^{-12}	-115	Sander et al. (2011)
OH + CH$_3$Cl → Cl + HO$_2$ + H$_2$O	3.90 x 10^{-12}	-1411	Sander et al. (2011)
OH + CH$_2$Cl$_2$ → 2 Cl + HO$_2$ + H$_2$O	1.90 x 10^{-12}	-870	Sander et al. (2011)
OH + CHCl$_3$ → 3 Cl + HO$_2$ + H$_2$O	2.20 x 10^{-12}	-920	Sander et al. (2011)
OH + Cl$_2$ → HOCl + Cl	2.60 x 10^{-12}	-1100	Sander et al. (2011)

Reaction	A	B	Reference
$OH + Cl_2O_2 \rightarrow HOCl + ClOO$	6.00×10^{-13}	670	Sander et al. (2011)
$OH + ClNO_2 \rightarrow HOCl + NO_2$	2.40×10^{-12}	-12 50	Sander et al. (2011)
$OH + ClNO_3 \rightarrow HOCl + NO_3$	1.20×10^{-12}	-330	Sander et al. (2011)
$OH + ClO \rightarrow HCl + O_2$	6.00×10^{-13}	230	Sander et al. (2011)
$OH + ClO \rightarrow HO_2 + Cl$	7.40×10^{-12}	270	Sander et al. (2011)
$OH + HCl \rightarrow H_2O + Cl$	1.80×10^{-12}	-250	Sander et al. (2011)
$OH + HOCl \rightarrow H_2O + ClO$	3.00×10^{-12}	-500	Sander et al. (2011)
$OH + OClO \rightarrow HOCl + O_2$	1.50×10^{-12}	600	Sander et al. (2011)
$Cl + CH_4 \rightarrow HCl + CH_3O_2$	9.60×10^{-12}	-1360	Atkinson et al. (2004)
$Cl + C_2H_4 \rightarrow HCl + C_2H_5O_2$	1.00×10^{-10}		Lurmann et al. (1986)
$Cl + CH_2O \rightarrow HCl + HO_2 + CO$	8.10×10^{-11}	-30	Sander et al. (2003)
$Cl + PAN \rightarrow HCl + CH_2O + NO_3$	1.00×10^{-14}		Sander et al. (2003)
$Cl + HNO_3 \rightarrow HCl + NO_2$	1.00×10^{-16}		Sander et al. (2003)
$Br + O_3 \rightarrow BrO + O_2$	1.60×10^{-11}	-780	Sander et al. (2011)
$Br + HO_2 \rightarrow HBr + O_2$	4.80×10^{-12}	-310	Sander et al. (2011)
$Br + CH_2O \rightarrow HO_2 + CO + HBr$	1.70×10^{-11}	-800	Sander et al. (2011)
$Br + C_2H_6 \rightarrow C_2H_5O_2 + HBr$	2.36×10^{-10}	-6411	Seakins et al. (1992)
$Br + C_3H_8 \rightarrow C_3H_7O_2 + HBr$	8.77×10^{-11}	-4330	Seakins et al. (1992)
$Br + CH_3CHO \rightarrow CH_3CO_3 + HBr$	1.30×10^{-11}	-360	Atkinson et al. (2007)
$Br + CH_3COCH_3 \rightarrow PROPAO_2 + HBr$	1.66×10^{-10}	-7000	King et al. (1970)
$Br + C_3H_6 \rightarrow PROPEO_2 + HBr$	3.60×10^{-12}		Atkinson et al. (2006)
$Br + ALKEN \rightarrow ALKENO_2 + HBr$	3.60×10^{-12}		Atkinson et al. (2006)
$Br + BrNO_3 \rightarrow Br_2 + NO_3$	4.90×10^{-11}		Orlando and Tyndall (1996)
$Br + NO_3 \rightarrow BrO + NO_2$	1.60×10^{-11}		Sander et al. (2011)
$HBr + OH \rightarrow Br + H_2O$	5.50×10^{-12}	200	Sander et al. (2011)
$BrO + OH \rightarrow Br + HO_2$	1.70×10^{-11}	250	Sander et al. (2011)
$BrO + HO_2 \rightarrow HOBr + O_2$	4.50×10^{-12}	460	Sander et al. (2011)
$BrO + NO \rightarrow Br + NO_2$	8.80×10^{-12}	260	Sander et al. (2011)
$BrO + BrO \rightarrow 2 Br + O_2$	2.40×10^{-12}	40	Sander et al. (2011)
$BrO + BrO \rightarrow Br_2 + O_2$	2.80×10^{-14}	860	Sander et al. (2011)
$Br_2 + OH \rightarrow HOBr + Br$	2.10×10^{-11}	240	Sander et al. (2011)
$CHBr_3 + OH \rightarrow 3 Br + CO$	1.35×10^{-12}	-600	Sander et al. (2011)
$CH_2Br_2 + OH \rightarrow 2 Br + CO$	2.00×10^{-12}	-840	Sander et al. (2011)
$CH_3Br + OH \rightarrow Br + CO$	2.35×10^{-12}	-1300	Sander et al. (2011)
$I + O_3 \rightarrow IO + O_2$	2.10×10^{-10}	-830	Atkinson et al. (2007)
$I + HO_2 \rightarrow HI + O_2$	1.50×10^{-11}	-1090	Sander et al. (2011)
$I_2 + OH \rightarrow HOI + I$	2.10×10^{-10}		Atkinson et al. (2007)
$HI + OH \rightarrow I + H_2O$	1.60×10^{-11}	440	Atkinson et al. (2007)
$HOI + OH \rightarrow IO + H_2O$	5.00×10^{-12}		Riffault et al. (2005)
$IO + HO_2 \rightarrow HOI + O_2$	1.40×10^{-11}	540	Atkinson et al. (2007)
$IO + NO \rightarrow I + NO_2$	7.15×10^{-12}	300	Atkinson et al. (2007)
$CH_3I + OH \rightarrow H_2O + I$	4.30×10^{-12}	-112 0	Atkinson et al. (2008)
$INO + INO \rightarrow I_2 + 2 NO$	8.40×10^{-11}	-2620	Atkinson et al. (2007)
$INO_2 + INO_2 \rightarrow I_2 + 2 NO_2$	4.70×10^{-12}	-1670	Atkinson et al. (2007)
$I_2 + NO_3 \rightarrow I + INO_3$	1.50×10^{-12}		Atkinson et al. (2007)
$INO_3 + I \rightarrow I_2 + NO_3$	9.10×10^{-11}	-146	Kaltsoyannis and Plane (2008
$OIO + OIO \rightarrow I_2O_4$	1.50×10^{-10}		Gómez Martin et al. (2007)
$OIO + NO \rightarrow NO_2 + IO$	1.10×10^{-12}	542	Atkinson et al. (2007)
$IO + IO \rightarrow I + OIO$	2.16×10^{-11}	180	Atkinson et al. (2007)
$IO + IO \rightarrow I_2O_2$	3.24×10^{-11}	180	Atkinson et al. (2007)
$IO + OIO \rightarrow I_2O_3$	1.50×10^{-10}		Gómez Martin et al. (2007)

Reaction			Reference
$I_2O_2 \rightarrow IO + IO$	$1.00 \times 10^{+12}$	-9770	Ordóñez et al. (2012)
$I_2O_2 \rightarrow OIO + I$	$2.50 \times 10^{+14}$	-9770	Ordóñez et al. (2012)
$I_2O_4 \rightarrow 2\ OIO$	3.80×10^{-02}		Kaltsoyannis and Plane. (2008)
$INO_2 \rightarrow I + NO_2$	$9.94 \times 10^{+17}$	-11859	McFiggans et al. (2000)
$INO_3 \rightarrow IO + NO_2$	$2.10 \times 10^{+15}$	-13670	Kaltsoyannis and Plane. (2008)
$IO + ClO \rightarrow I + OClO$	2.59×10^{-11}	280	Atkinson et al. (2007)
$IO + ClO \rightarrow I + Cl + O_2$	1.18×10^{-12}	280	Atkinson et al. (2007)
$IO + ClO \rightarrow ICl + O_2$	9.40×10^{-13}	280	Atkinson et al. (2007)
$I + BrO \rightarrow IO + Br$	1.20×10^{-11}		Sander et al. (2011)
$IO + Br \rightarrow I + BrO$	2.70×10^{-11}		Bedjanian et al. (1997)
$IO + BrO \rightarrow Br + I + O_2$	3.00×10^{-12}	510	Atkinson et al. (2007)
$IO + BrO \rightarrow Br + OIO$	1.20×10^{-11}	510	Atkinson et al. (2007)
$ClO + BrO \rightarrow OClO + Br$	1.60×10^{-12}	430	Atkinson et al. (2004)
$ClO + BrO \rightarrow Br + Cl + O_2$	2.90×10^{-12}	220	Atkinson et al. (2004)
$ClO + BrO \rightarrow BrCl + O_2$	5.80×10^{-13}	170	Atkinson et al. (2004)

145

Table 4. Termolecular halogen reactions included in the scheme. This includes reactions from previous updates to halogen chemistry in GEOS-Chem (Parrella et al., 2012; Eastham et al., 2014; Schmidt et al., 2016; Sherwen et al., 2016a; Sherwen et al., 2016b). The lower pressure limit rate (k0) is given by $A_0(\frac{300}{T})^x$. The high pressure limit is given by $k\infty$. Fc characterizes the fall off curve of the reaction as described by Atkinson et al. (2007).

Termolecular reaction	A_0 (molecules^{-2}cm^{6}s^{-1})	x	k_∞	m	Fc	Reference
$Cl + O_2 + M \rightarrow ClOO$	2.20×10^{-33}	0	1.80×10^{-10}	3.1	0.6	Sander et al. (2011)
$ClO + ClO + M \rightarrow Cl_2O_2$	1.60×10^{-21}	2	3.0×10^{-12}	4.5	0.6	Sander et al. (2011)
$ClO + NO_2 + M \rightarrow ClNO_3$	1.80×10^{-31}	3.4	1.50×10^{-11}	1.9	0.6	Sander et al. (2011)
$ClOO + M \rightarrow Cl + O_2$	3.30×10^{-9}	0	2.73×10^{14}	3.1	0.6	Sander et al. (2011)
$Cl_2O_2 + M \rightarrow Cl + O_2$	9.30×10^{-6}	2	1.74×10^{15}	4.5	0.6	Sander et al. (2011)
$Cl + C_3H_6 + M \rightarrow ALKANO_2$	4.0×10^{-28}	0	2.80×10^{-10}	-	0.6	Atkinson et al. (2006)
$Br + NO_2 + M \rightarrow BrNO_2$	4.20×10^{-31}	2.4	2.70×10^{-11}	-	0.6	Sander et al. (2011)
$BrO + NO_2 + M \rightarrow BrNO_3$	5.20×10^{-31}	3.2	6.90×10^{-12}	-	0.6	Sander et al. (2011)
$I + NO + M \rightarrow INO$	1.80×10^{-32}	1	1.70×10^{-11}	-	0.6	Atkinson et al.(2007)
$I + NO_2 + M \rightarrow INO_2$	3.0×10^{-31}	1	6.60×10^{-11}	-	0.63	Atkinson et al.(2007)
$IO + NO2 + M \rightarrow INO_3$	7.70×10^{-31}	5	1.60×10^{-11}	-	0.4	Atkinson et al.(2007)

150

Table 5. Halogen multiphase reactions and reactive uptake coefficients (γ).

Reaction	Reactive uptake coefficient on sea salt (γ)	Reactive uptake coefficient on sulfate aerosols (γ)	Reference
$HOBr + HBr \rightarrow Br_2 + H_2O$[g]	0.2	0.2	Parrella et al. (2012)
$HOBr + HCl \rightarrow BrCl + H_2O$	0.2	0.2	Sander et al. (2011)
$ClNO_3 + HBr \rightarrow BrCl + HNO_3$	0.2	0.2	Compromise between Sander et al. (2011) and Badia et al. (2019)
$ClNO_3 \rightarrow HOCl + HNO_3$	0.001[a] 0.01[b]	0.001[a] 0.01[b]	Badia et al. 2019
$BrNO_3 \rightarrow HOBr + HNO_3$	0.03[a] 0.8[b]	0.03[a] 0.8[b]	Badia et al. 2019

Reaction			
$I_2O_x \rightarrow 2\ I_{aer}$	0.02	2.10^{-2}	Sherwen et al. 2016
$HI \rightarrow I_{aer}$	0.1	-	Sherwen et al. 2016
$HOI \rightarrow 0.85\ ICl + 0.15\ IBr + HNO_3$	0.01	-	Sherwen et al. 2016
$INO_3 \rightarrow 0.85\ ICl + 0.15\ IBr + HNO_3$	0.01	-	Sherwen et al. 2016
$INO_2 \rightarrow 0.85\ ICl + 0.15\ IBr + HNO_3$	0.02	-	Sherwen et al. 2016
$N_2O_5 \rightarrow 1.5\ HNO_3 + 0.5\ ClNO_2$	3.10^{-2}	-	Hossaini et al. 2016

[a]Uptake coefficient for moderate temperatures.

[b]Uptake coefficient for cold temperatures.

[c] For second order reaction, rate constants are calculated by assuming that the first reactant is limiting thus, the first-order rate constant is divided by the concentrations of the adsorbed species.

2.2 Simulations

For these developments, LMDZ-INCA is used with a 3.75 ° × 1.9 ° resolution over 39 vertical layers. This resolution, coarser than the resolution now commonly used in the CMIP6 model exercise, was the standard LMDZ resolution for CMIP5 and allows faster simulations necessary in model development. The LMDZ wind fields and sea surface temperature are nudged on ECMWF reanalysis for the year 2010 in all simulations. The aerosol distribution and monthly variations used for heterogeneous reactions calculations are specified from climatologies precomputed with another version of the same model but with fully interactive calculations of aerosols. All simulations cover 1 year (2010), and follow a spin-up period of one year. Three types of simulations have been performed to simulate (i) present-day conditions, (ii) preindustrial conditions, and (iii) sensitivity to ozone precursors. For sensitivity tests, simulations with individual emission perturbations of photooxidant precursors (-20%) of NO_x, CO and NMVOCs and concentration reduction (-20%) of CH_4, were performed. For each type of simulation, two versions of the model are applied: one accounting for the halogen chemistry (called Halo simulations hereafter) and a reference simulation without halogen chemistry called "NoHalo".

2.2.1 Present-day set-up

Primary halogenated compounds can originate from both inorganic and organic sources. Inorganic species are reactive species emitted by different sources (e.g. oceans, sea salts), but also result from atmospheric reactions (Simpson et al., 2015). Organic species are only of primary origin and are photooxidized in the atmosphere to form halogen radicals (Simpson et al., 2015). Table 6 shows the emissions of halogenated compounds as considered in INCA. Organo-bromines (e.g. $CHBr_3$, CH_2Br_2), organo-iodines (e.g. CH_3I, CH_2I_2) and interhalogen species (e.g. CH_2IBr, CH_2ICl) are those used by the CAM-Chem model (Ordóñez et al., 2012).

Sources of organic chlorine are diverse, mainly originating from biological activity on the surface of the oceans and from forest fires. The emissions of these chlorocarbons are detailed in Table S2. In INCA, inorganic chlorine, HCl - the major reservoir of chlorine in the atmosphere - is considered as being emitted by sea salts (90 000 Gg Cl.yr^{-1}) and by forest fires (6400 Gg Cl.yr^{-1}) with total based on Lobert et al., 1999 and Hossaini et al., 2016. Note that more comprehensive but hard to implement approaches relying on pH dependent parameterization of the dechlorination of sea salts have been recently implemented in GEOS-Chem. HCl emissions from industrial sources (McCulloch et al., 1999) are neglected as recommended by Wang et al. (2019), to avoid overestimating HCl in urban areas. $ClNO_2$ is emitted by the heterogeneous reaction of N_2O_5 on sea salts and produces 2217 Gg Cl.yr^{-1}.

CH₃Br emissions are from oceanic origin (40%) and from agriculture (60%) (Barker et al., 2016) and represent 91 Gg of Br.yr⁻¹ (Schmidt et al. (2016). IBr and ICl originate from the heterogeneous reaction of HOI, INO_2 and INO_3 on sea salt aerosols (Table 5) as considered in other models (Saiz-Lopez et al., 2014; Sherwen et al., 2016b), but without accounting for pH dependence (McFiggans et al., 2000).

The inorganic iodine distribution of emissions (HOI and I_2) are prescribed from Prados-Roman et al., (2015a) and have been computed by the CAM-Chem model considering sea-air fluxes as a function of the oxidation of aqueous iodide by atmospheric ozone on the ocean surface (Carpenter et al., 2013; MacDonald et al., 2014), the deposition of ozone to the ocean surface, the sea surface temperature and the wind speed (Prados-Roman et al., 2015b).

2.2.2 Preindustrial set-up

The aim of this simulation is to explore how the sensitivity of ozone to anthropogenic emissions perturbations changes since the preindustrial period. Only emissions from natural sources are included for the simulation of the preindustrial troposphere, following the approach used by other modelling teams to quantify this perturbation. Emissions of halogenated compounds from biomass burning are reduced to 10% of their current values (Wang and Jacob, 1998). The methane concentration is set at 700 ppbv (IPCC, 2014).

Organo-iodine emissions are almost unchanged between the PI and PD. For organo-bromines, CHBr₃ and CH₂Br₂ preindustrial emissions are equivalent to the PD ones, following the methodology of Parrella et al. (2012). The concentration of CH₃Br is set to ~ 5 ppbv is considered in agreement with the measurements from ice cores (Saltzman et al., 2004). Preindustrial emissions of CH₃Cl, CHCl₃ and CH₂Cl₂ (see table S2) are taken from (Carpenter et al., 2014; Hu, 2012; Montzka et al., 2011; Worton et al., 2006). HOI and I_2 emissions are ~ 40% lower than today because they are sensitive to atmospheric ozone content which was lower in the pre-industrial era (Prados-Roman et al., 2015a; Sherwen et al., 2017). Global emissions for each primary halogenated compound are reported in Table 6.

Table 6: Emission of halogen gases for preindutrial and present-day simulations. Sources of organic species (CH₃X, CH₂X₂, CHX₃) are shown in terms of emissions. I₂ and HOI are the inorganic oceanic source that depends on surface ozone (Carpenter et al., 2013). IBr and ICl is released following gaseous iodine uptake on sea salt. ClNO₂ is emitted by absorption of N₂O₅ on sea salt.

Compounds	I (Tg I.an⁻¹)		Br (Tg Br.an⁻¹)		Cl (Tg Cl.an⁻¹)	
	Preindustrial	Present	Preindustrial	Present	Preindustrial	Present
CH₃X	209	219	36	91	2081	2166
CH₂X₂	108	108	62	62	199	628
CHX₃	-	-	506	506	236	315
HOI	1361	2448	-	-	-	-
I₂	34	59	-	-	-	-
ClNO₂	-	-	-	-	169	2217
CH₂IBr	50	50	32	32	-	-
CH₂ICl	168	168	-	-	47	47
IBr, ICl	-	-	495	799	1244	2008
HCl	-	-	-	-	96429	96429
Total	**1930**	**3052**	**1131**	**1490**	**100406**	**103810**

3 Evaluation of the representation of the halogen-driven ozone sinks

We first assess the ozone sensitivity to halogen chemistry in LMDZ-INCA, then we evaluate the performance of the model in simulating the climatologies of halogen species which are important for the global ozone loss. In order to do so, model outputs for compounds of interest in this chemistry are compared to a range of halogen observations and simulations from other models with halogen chemistry. An analysis of the model tropospheric budgets of key halogen species is also performed.

3.1 Impact on ozone loss in present-day

215 Table 7 presents the ozone budget in LMDZ-INCA with and without consideration of halogen chemistry. Overall, when halogens are considered, the tropospheric ozone burden is reduced by 22% for present-day conditions which is in the 5 to 25% range reported from other models which include for Cl, Br and I chemistry (Saiz-Lopez et al., 2012; Saiz-Lopez et al., 2015, 2012a; Sherwen et al., 2016b; Badia et al., 2019). Over the global troposphere, it is associated to a decrease of the annual-average ozone mixing ratio (mass-weighted) of ozone of 9.7 ppbv (compared to 9.4 ppbv in GEOS-Chem, Sherwen et al.,
220 2016b). Over the tropospheric tropical column, the annual-average ozone mixing ratio (mass-weighted) decreases by 8 ppbv (21%) which is twice as large as the relative change reported in Saiz-Lopez et al. (2014). Surface ozone averaged over continental areas undergoes a decrease of 6 ppbv (23%) while surface ozone in oceanic areas, where the majority of primary halogenated compounds are emitted, decreases by 7.7 ppbv (32%) (range reported in other studies is 20-33%; Saiz-Lopez et al., 2014; Long et al., 2014; Prados-Roman et al., 2015a; Sherwen et al., 2016b).

225 Figure 2 shows the absolute changes in surface ozone and relative change in zonally-averaged ozone in a simulation with halogen chemistry relative to a simulation without it. Significant relative losses are found in the Southern Hemisphere, which are due to the strong emissions of halogenated species from the ocean in this region (Long et al., 2014; Saiz-lopez et al., 2012; Schmidt et al., 2016; Sherwen et al., 2016b, 2016a). Most of the change in total tropospheric ozone concentration occurs in the free troposphere between 350 hPa and 900 hPa (63%). This result is similar in magnitude to the relative change reports in
230 GEOS-Chem (65%; Sherwen et al., 2016b) and CAM-Chem (65%; Iglesias-Suarez et al., 2020).
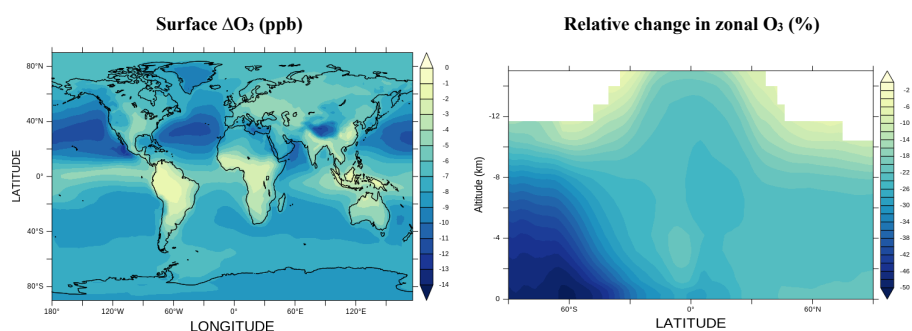
Figure 2: Surface ozone changes (ppbv) and relative change in zonal tropospheric ozone (%) between simulations with and without halogen chemistry.

The annual production of ozone decreases by 4.7% when the chemistry of halogens is considered. This decrease is due to a
235 reduction in NO_x concentrations of 32.8% (Table 7) due to the hydrolysis of XNO_3 (X = Cl, Br, I) leading to deposition losses, in accordance with previous studies (Saiz-Lopez et al., 2012b; Long et al., 2014; von Glasow et al., 2004; Parrella et al., 2012; Schmidt et al., 2016, Sherwen et al., 2016b).

The vertical profile of the different contributions to chemical ozone loss is shown Figure 3. The processes leading to ozone loss differ considerably between simulations with and without halogenated compounds (Table 7). Halogens account for nearly
240 ~22% of the ozone loss in the boundary layer in the halogen simulation, as shown in Fig. 3. Halogens represent 55% of the Ox loss in the upper troposphere (350 hPa > pressure > tropopause) while this value is about 33% and 40% in GEOS-Chem with the iodine+bromine, and the iodine+bromine+chlorine chemistry, respectively. Such differences could be partly due to

differences in convection schemes which induce different uplifts of IO in the upper troposphere resulting in different IO concentrations (see section 3.1.3 below).

245 When chemistry of halogenated compounds is considered, the total annual chemical ozone loss decreases by 2.4% (Table 7). The relative contributions of different halogens to ozone loss are very similar to those of GEOS-Chem in Sherwen et al. (2016a). The loss of ozone by chlorine, bromine and iodine represents 0.5%, 4.7% and 18% of the total losses, respectively; thus, halogens represent 23.2% of the total loss of ozone. The sum of the ozone loss caused by the halogens is 984 Tg.yr^{-1}. Iodine is responsible for 78% of that halogen-mediated loss, while bromine accounts for 19%, which is close to the values

250 reported by Iglesias-Suarez et al., 2020 (80%, 16% respectively). Iodine is responsible for an overall tropospheric ozone loss of 762 Tg.yr^{-1} (comparable to the 748 Tg.yr^{-1} reported by Sherwen et al., 2016a). Much of this loss arises from the photolysis of HOI after its production from the reaction of IO with HO$_2$ and the photolysis of OIO after its production from reactions implicating IO and I$_x$O$_y$. Bromine is responsible for an overall tropospheric loss of 187 Tg.yr^{-1} which mostly arises from the photolysis of HOBr after its production from the reaction of BrO with HO$_2$.
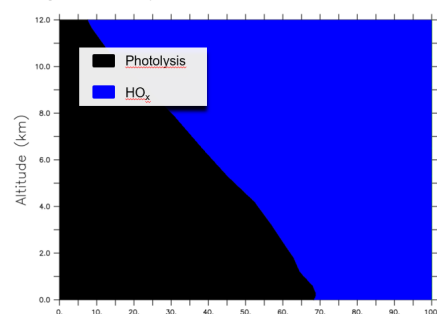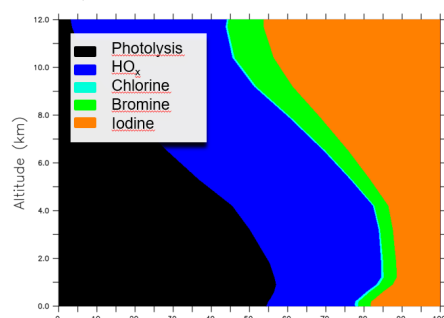
255 **Figure 3: Contribution of the chemical ozone sinks as a function of the altitude without (left) and with (right) consideration of the chemistry of halogens in LMDZ-INCA.**

The inclusion of halogens leads to an overall decrease in the net production of tropospheric ozone (PO$_3$-LO$_3$) of 20% (126 Tg.yr^{-1}). Consequently, the lifetime of ozone is significantly decreased by 3.2 days and reaches 17.9 days.

Table 7: Comparison of global tropospheric O$_x$ budgets of "Halo" and "NoHalo" simulations in INCA for the PI and PD.

	Preindustrial Halo	Preindustrial NoHalo	Present day Halo	Present day NoHalo
Ozone burden (Tg)	170.7	218.9	249.9	317
Ozone chemical sources (Tg.yr^{-1})				
NO + HO$_2$	1459	1554	2954	3190
NO + CH$_3$O$_2$	474.9	477.2	1134	1159
NO + RO$_2$	380.7	355.5	625.8	596.7
Total chemical ozone sources (PO$_3$)	**2314**	**2387**	**4714**	**4946**
Ozone chemical sinks (Tg.yr^{-1})				
O$_3$ + H$_2$O → 2 OH + O$_2$	1099	1497	1905	2460
O$_3$ + HO$_2$ → OH + O$_2$	431.5	648	917	1295
O$_3$ + OH → HO$_2$ + O$_2$	207.1	297.8	349.4	488.7
Bromine O$_3$ sinks	155.3	-	186.9	-

Iodine O$_3$ sinks	536.9	-	762.3	-
Chlorine O$_3$ sinks	23.51	-	22.16	
Other O$_3$ sinks	78.06	85.11	88.5	92.87
Total chemical ozone sink (LO$_3$)	**2531**	**2528**	**4231**	**4337**
Ozone PO$_3$-LO$_3$ (Tg.yr^{-1})	-216.6	-141	483	609.1
Ozone dry deposition (Tg.yr^{-1})	403.4	593.4	875.5	1139
Ozone lifetime (days)	21.2	25.6	17.9	21.1
Ozone STE (PO$_3$-LO$_3$-Dry dep) (Tg.yr^{-1})	-620	-734.5	-392.4	-530.2

260

3.2 Present-day budgets for halogenated species in LMDZ-INCA

In order to reflect the role played by the halogenated species in their respective cycle, inorganic halogens are presented hereafter under the name X$_y$ which can be divided into HX and X*. HX in LMDZ-INCA takes part in heterogeneous bimolecular reactions. In CAM-Chem and GEOS-Chem, the representation of this chemistry is more detailed: HX can

265 associated with chemistry on droplets or particles and dissociate (Fernandez et al., 2014b; Ordóñez et al., 2012; Prados-Roman et al., 2015a; Saiz-Lopez et al., 2012b, 2014, 2015), also in GEOS-Chem described in Sherwen et al. (2016b). X* is subdivided into: the "reactive halogen" XO$_x$, grouping X + XO*, and the reservoir species X$_2$, HOX, XNO$_2$, XNO$_3$ and which have a relatively longer lifetime. These last species are formed mostly at night and serve as reservoirs of reactive halogens far from its primary sources.

270 In the following subsections, we present, for each halogen, the species considered in each reservoir, their respective tropospheric mass burden and the main fluxes between these reservoirs. The purpose is to evaluate the representation of halogenated species of interest for ozone and to discuss the limitations of the model in the computation of the budget of each halogen family.

3.2.1 Iodine

275 Iodine chemistry is the most impactful with regard to the ozone loss. The simplified iodine cycle is shown schematically in Fig. 4. The burden of inorganic iodine excluding IBr / ICl and iodine in aerosols is ~ 22.0 Gg in the troposphere in LMDZ-INCA, comparable to the value of ~ 27.9 Gg reported by Sherwen et al. (2016b, Figure 7). HOI and OIO species, whose photolysis result in atomic iodine production, are the main intermediates for direct ozone loss. HOI is the most abundant iodine species and its wet deposition controls the total atmospheric iodine burden. Its tropospheric burden of 12.8 Gg I in INCA is

280 very close to the 13 Gg simulated by Sherwen et al., 2016a. The tropospheric burden of OIO in INCA, 0.43 Gg I, is comparable to the 0.55 Gg I also reported in Sherwen et al., 2016a. Overall, the global levels of HOI and OIO, simulated by INCA are similar to their simulation by other models described in the literature.

The tropospheric burdens of HI, INO$_2$, and I$_2$ sum up to 1 Gg I, lower than the burdens reported for GEOS-Chem and totaling 2.48 Gg I (Sherwen et al., 2016a). The global burden of I$_2$ in INCA is lower than that in GEOS-Chem (Sherwen et al. 2016a)

285 because in Sherwen et al. (2016a), heterogeneous reactions transform INO$_3$, INO$_2$ and HOI into I$_2$, whereas in INCA, these reactions produce IBr and ICl, similarly to the heterogeneous reactions adopted by Sherwen et al., (2016b). Other quantifications in the literature are lacking to explain the differences in INO$_2$ and HI, however, Saiz-Lopez et al. (2014) indicate that minor iodine species (I$_{min}$ = HI + OIO + INO$_2$ + INO) represent less than 5% of the mass in tropospheric inorganic iodine (2.3% in our case). In INCA, the tropospheric I$_y$ mean is 1.3 pptv, whereas previous model studies found a range of ~ 0.5 to 1

290 pptv (Saiz-Lopez et al., 2014; Sherwen et al., 2016a, 2016b). A large set of observations has been assembled by Sherwen et al. (2016a) for IO. Measurements of IO during oceanic campaigns show a strong diurnal variation (IO being present only during day time) with climatological concentrations (local observations averaged over 20° bins) comprised between 0.3 and 1 pptv. These IO concentrations show a weak latitudinal variability and a rapid decrease with altitude to reach values of about

0.2 pptv from 2km to the tropopause (observations gathered and reported by Sherwen et al. 2016a). Surface values simulated
by INCA agree within a factor of two with these observations. Over oceans, the annual mean surface concentrations of IO is
approximately 0.2 pptv with concentrations comprised between 0. and 2. pptv. This is similar to the range simulated by
Sherwen et al. (2016a) (0.25 - 1 pptv) and to the observations reported by Prados-Roman et al. (2015). Concentrations over
oceans are comprised between In the tropics (20° S – 20° N), levels of surface IO in INCA (0.35 pptv) are in agreement with
model results reported for CAM-Chem (~0.4 ppt) (Saiz-Lopez et al., 2014). In the free troposphere, IO levels slightly increase
with altitude to reach diurnal values of ~0.5 pptv at 10km in INCA. This overestimation of IO in the upper troposphere is
common to all current models simulation iodine and remain unclear (Sherwen et al. 2016a, Badia et al. 2019). A study
conducted by Saiz-Lopez et al. (2015) indicates that inclusion of HOI and INO_3 recycling on sea ice crystals is capable of
reproducing free- and upper-tropospheric IO levels.

The IO_x family influences the oxidative capacity of the troposphere through the catalytic cycles of ozone depletion (Brasseur,
2005), modifies the HO_x (HO_2 / OH) and NO_x (NO_2 / NO) ratios (Bloss et al., 2010), produces photolabile higher order iodine
oxides (I_xO_y) (Gómez Martín et al., 2020; Lewis et al., 2020) and generates different forms of inorganic iodine (Saiz-Lopez et
al., 2012a). For that reason, a correct representation of the branching ratios and the generation and loss of IO_x is crucial.
Globally, IO_x production in INCA is dominated by inorganic photolysis of HOI (80.5%), OIO (10.2%), INO_3 (5.4%) and I_2O_x
(3.9%). This partition is comparable to the one reported in Sherwen et al., 2016b who found a 76% HOI photolysis contribution
and a 11% OIO photolysis contribution. The main IO_x loss pathway is the production of HOI by IO reaction with HO_2 (78.5%),
with additional loss pathways by self-reaction, reaction with NO_x and BrO contributing 11.3%, 5.7% and 4.5%, respectively
– numbers that are very close to the branching ratios reported in Sherwen et al., 2016b (77%, 10%, 7.7% and 4.6%
respectively).
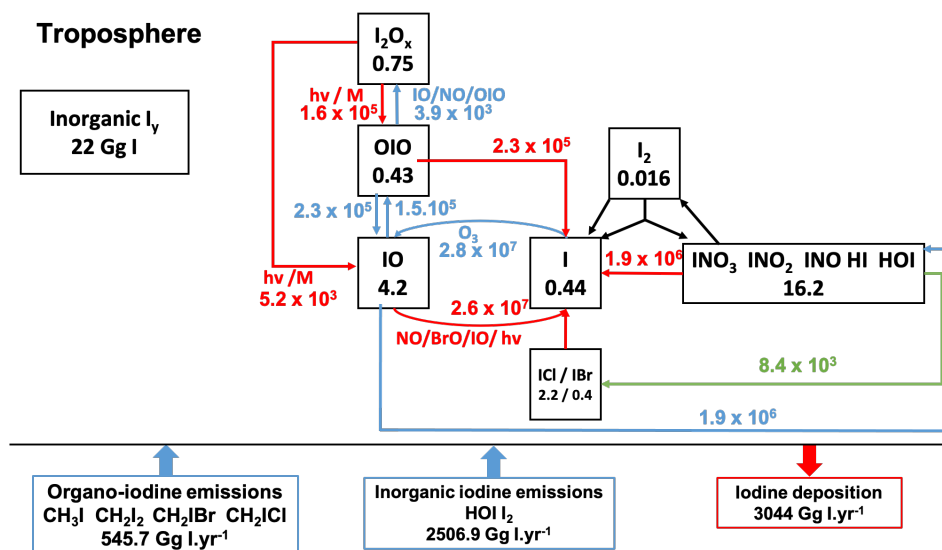
**Figure 4: Iodine budget in the present-day reference simulation with simplified cycle of tropospheric I_y species. Heterogeneous
reactions are shown in green. Photolysis reactions are in red. The numbers in the boxes represent the mass balance of the species
families in Gg I.**

3.2.2 Bromine

The tropospheric bromine budget and simplified recycling cycle are illustrated in Fig. 5. The tropospheric inorganic bromine burden is ~ 27 Gg in LMDZ-INCA, close to the 28 Gg reported for the most recent version of GEOS-Chem (Wang et al., 2021). On an annual average, INCA simulates daytime BrO values in the free troposphere of ∼0.3 pptv within the tropics, close to the results in CAM-Chem (~0.2 pptv) (Fernandez et al., 2014). At the tropical tropopause layer, the modeled tropical BrO concentrations in INCA are ~3 pptv, close to the CAM-Chem modelling result of 2.0±1.5 pptv and the observed concentrations of 3.2±1.6 pptv (Fernandez et al., 2014a). Overall, the global tropospheric mean of BrO simulated by INCA is 0.6 pptv (in agreement with model results from Parrella et al. (2012)) but is in the lower end of the 0.5 to 2 pptv range inferred from observations (Dorf et al., 2008; Saiz-Lopez and von Glasow, 2012, Stone et al., 2012).

In this first implementation of halogen chemistry in a version of LMDz-INCA, the focus is on gaseous chemistry. Aqueous chemistry in droplets or on ice crystals in clouds is not accounted for in the first version of the scheme because it is complex and uncertain, and, more importantly, might not be a dominant mechanism for global ozone loss. Nonetheless, the scheme includes recycling through heterogeneous chemistry on sea salt and sulfate aerosols. A study by Badia et al. (2019) using WRF-Chem shows that heterogeneous halogen chemistry (on all types of aerosols) allows a better vertical Br_y partitioning, but contributes little (~6%) to ozone loss compared to the gas-phase halogen chemistry (25%) on a global scale. Our choice to include, in this first step, reactions on sea salt and sulfate aerosols only, is suited to reproduce bromine-mediated ozone loss in the marine boundary layer but probably tends to slightly underestimate the halogen-mediated ozone loss in the global troposphere.

Due to this lack of in-cloud halogen chemistry in cloud droplets and ice crystals, whose importance increase with altitude, the bromine chemistry in INCA is less dynamic and the recycling of bromine is less efficient in LMDZ-INCA compared to those reported for some versions of GEOS-Chem (Parrella et al., 2012; Schmidt et al., 2016; Sherwen et al., 2016b; Zhu et al., 2019). Note, however, that the recently updated HOBr heterogeneous chemistry implemented in the most recent GEOS-Chem version (Wang et al., 2021) results in much slower recycling of HOBr in clouds and aqueous aerosols than previously calculated. This results in fluxes from heterogeneous reactions (specifically HOBr + HBr → Br_2 + H_2O and HOBr + HCl → BrCl + H_2O) that sum up to 32 500 Gg Br.yr^{-1} and which is smaller for example than our estimates of 86 000 Gg Br.yr^{-1} but remain in the same order of magnitude. Finally, our branching ratios are found to be consistent with those in Schmidt et al., (2016) and Wang et al., (2021). This leads us to conclude that, although LMDZ-INCA does not integrate the same degree of details in tropospheric halogen heterogeneous chemistry compared to its peers, global fluxes in the bromine cycle of INCA appears to be more comparable in terms of bromine cycle with to those in the newest version of GEOS-Chem (see the detailed bromine budget and cycle in Fig. S1) and CAM-Chem (Iglesias-Suarez et al., 2020), than fluxes in the older versions of GEOS-Chem (Parrella et al., 2012; Schmidt et al., 2016; Sherwen et al., 2016b; Zhu et al., 2019). All these estimates remain in the same order of magnitude but the range of fluxes illustrates the level of uncertainties on the strength of the halogen heterogeneous recycling.

a supprimé: a

a supprimé: a
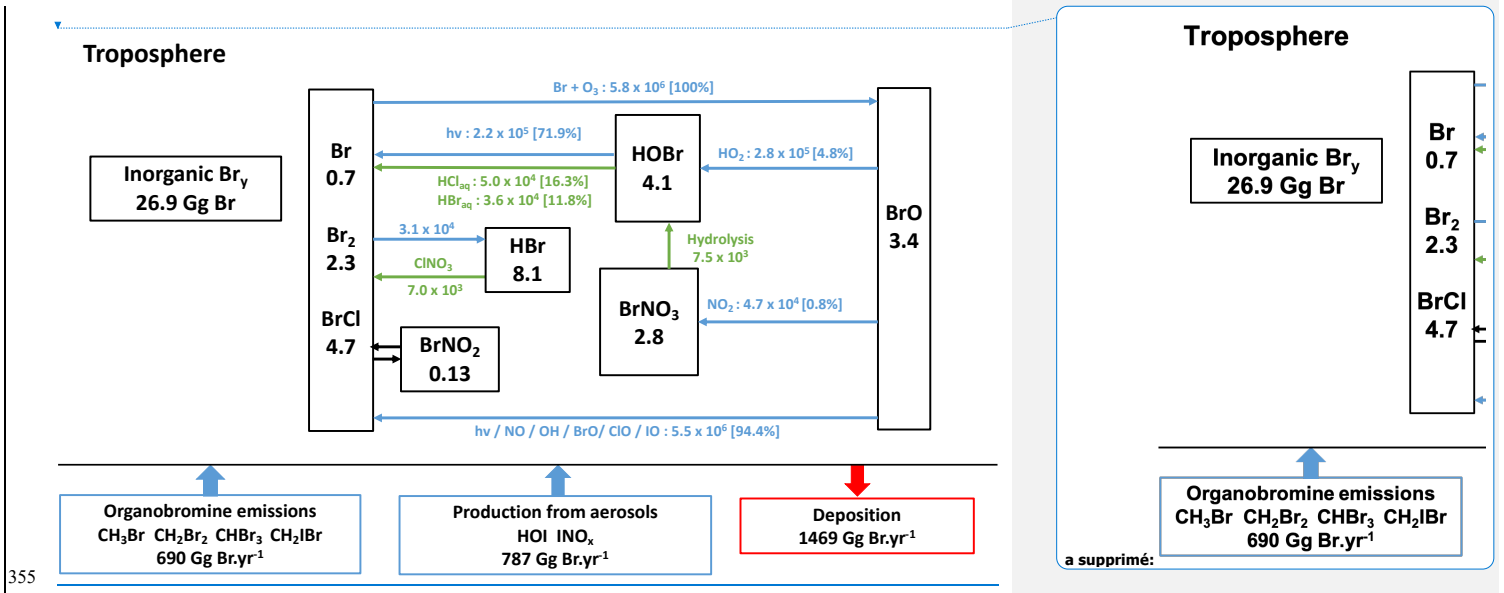
Figure 5: Bromine budget in the present-day reference simulation with a simplified representation of the cycle of tropospheric Br$_y$ species. Fluxes through the reactions, indicated next to the arrows, are in Gg Br.yr^{-1}. Heterogeneous reactions are represented in green. Percentages in brackets represent the branching ratios. The numbers in the boxes represent the burden of the species or families in Gg Br.

3.2.3 Chlorine

The total tropospheric burden of Cl$_y$ (inorganic chlorine) is 290 Gg of Cl, largely dominated by HCl. The total load of HCl is smaller than the one reported for GEOS-Chem (Wang et al., 2019) essentially because of the difference in the representation of the emissions. However, the total burden of reservoir species has a similar magnitude (10.4 Gg Cl). The halogen chemistry in INCA leads to a 25% higher quantity of available reactive chlorine compounds: Cl and ClO * (ClO* being ClO+ClOO+OClO+2 Cl$_2$O$_2$).

Atomic chlorine has two main chemical sinks. The first and most important in term of reaction flux, is the transformation of atomic Cl into ClO*. This conversion takes place mainly by reaction with ozone (99.5%), while the conversion of ClO$_x$ to Cl is dominated by reaction with NO (93.9%). The second path is represented by the chemical loss of reactive chlorine Cl to inactive chlorine HCl (Fig. 6), which is due to the reactions of Cl with methane and several NMVOCs. The conversion of Cl to ClO* is in strong competition with the second route. By dividing the fluxes of the conversion Cl to ClO* by the flux of conversion of Cl to HCl, we find that the chain length is short and equal to 1.3 (4.8×10^4 / 3.6×10^4). This is close to the chain length of 1.6 calculated by Wang et al. (2019) and shows that the branching ratios are in the same order of magnitude in both models, despite differences in NMVOC and CH$_4$ concentrations between the two models. Overall, we find that the partition between Cl and ClO* is correct in the model as well as the balance between radical and non-radical species although the latter is a little more shifted towards reactive species in INCA, compared to GEOS-Chem and CAM-Chem.

The average of climatological observations (mean over several months and representative of large areas) over 6 oceanic and coastal remote locations, shows a mean surface HCl mixing ratio of 196±114 pptv whereas INCA simulates an average of 193±98 ppt, compared to the 246±90 pptv in GEOS-Chem (Wang et al., 2019) (see Fig. S2). However, for continental regions,

LMDZ-INCA underestimates the HCl concentrations compared to observations, mainly because it does not include industrial emissions. $ClNO_2$ over continental areas does not exceed a few tens of ppt in INCA whereas observations at several continental locations, as gathered by Wang et al. 2019 (their Table 5), show concentrations of a few hundreds to thousands of ppts over

385 such locations for hourly maxima. This difference can arise from the coarse resolution of the model which does not resolve the spatial heterogeneity of these local observations (Sherwen et al., 2016b) and the absence of $ClNO_2$ production in sulphate-nitrate-ammonium aerosols (Wang et al., 2019). The chlorine Cl^* measurements to which we compare LMDZ-INCA results represent the sum of Cl_2, $HOCl$, $ClNO_2$, $ClNO_3$ and other minor components as explained in (Pszenny, 1993). LMDZ-INCA Cl^* values are of the same order of magnitude as measurements (see Table S3).

390
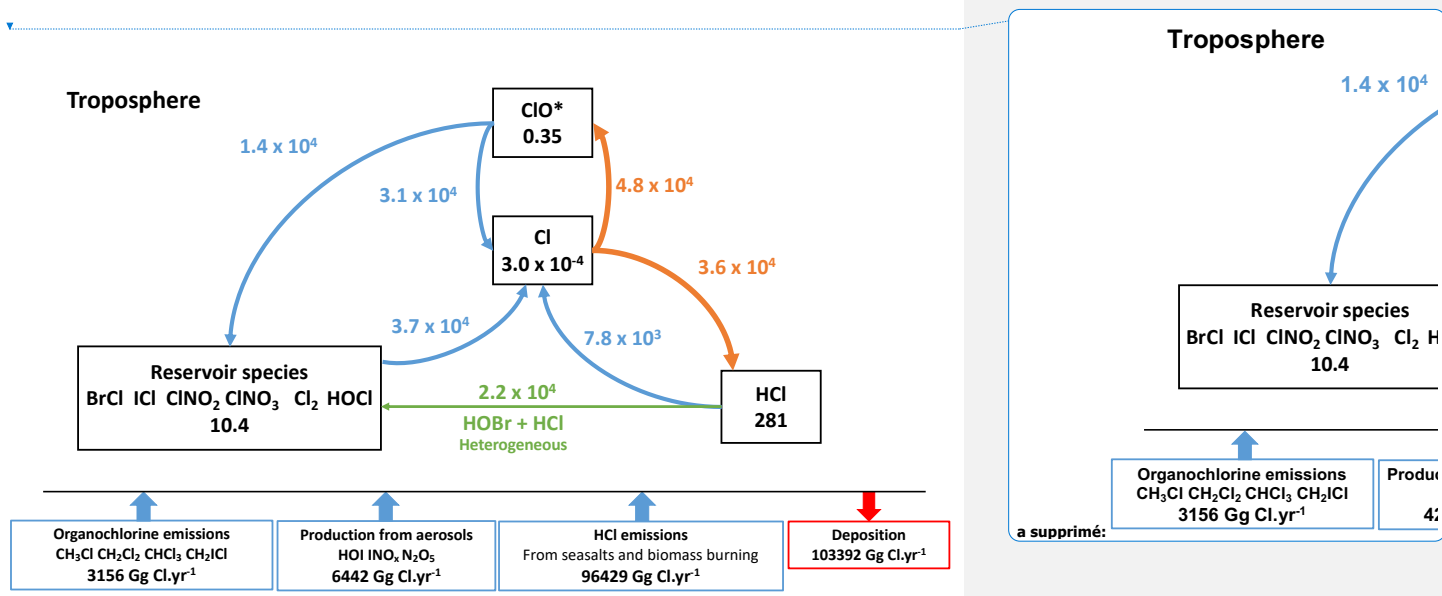
Figure 6: Simplified representation of the cycle of tropospheric Cl_y species in the reference simulation. Fluxes through the reactions
395 are in Gg Cl.yr^{-1}. Heterogeneous reactions are represented in green. The main loss pathways for atomic chlorine are in orange. The numbers in the boxes represent the mass balances of the species families in Gg Cl.

4 Perturbation of the ozone sensitivity to its precursors by halogen chemistry

In this section, the evolution of the model-calculated ozone sensitivity from the pre-industrial period to the present-day is assessed, with and without halogen chemistry, and compared with results from other models. Then the impact of halogen
400 chemistry on the sensitivity of ozone, OH radical and CH$_4$ concentrations to the emissions of anthropogenic ozone precursors is discussed.

4.1 Pre-industrial to present-day changes

With and without halogen chemistry, the model simulates significantly lower ozone concentrations in the pre-industrial compared to present due to the decrease in NO$_x$ concentrations. Taking into account halogen chemistry reduces the average
405 surface ozone concentrations for pre-industrial conditions by 5.0 ppbv (38%), with largest reductions over the oceans (5.5 ppbv, or 42.4%).

Globally, halogens reduce the tropospheric ozone burden by 67.1 Tg in present-day and 48.2 Tg in pre-industrial conditions (Table 7). Between PI and PD, ozone increases by 98.1 Tg (113 Tg in Sherwen et al., 2017) without halogen chemistry and by 79.2 Tg (90 Tg in Sherwen et al., 2017) with halogen chemistry. Both in PD and PI, halogens are responsible for about 23-28% of the ozone destruction. Tropospheric ozone lifetimes drop from 21.1 to 17.9 days in the present with the inclusion of halogens and from 25.6 to 21.2 days in the pre-industrial. The sensitivity of the burden of ground-level ozone to pre-industrial – present changes is ~ 20% lower when the chemistry of the halogens is considered. The changes observed in LMDZ-INCA and schematized in Fig. 7 are in agreement with the changes in Sherwen et al. (2017).
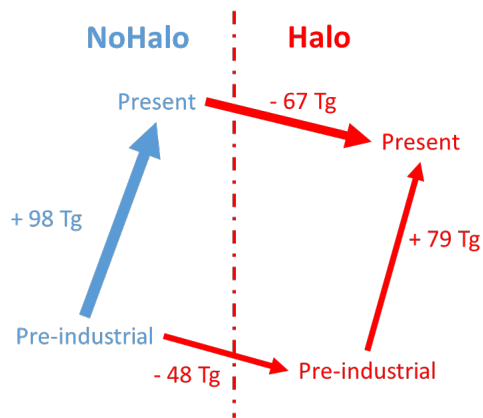
Figure 7: Schematic representation of the evolution of ozone mass budget changes between PI and PD, following the inclusion of halogen chemistry in LMDZ-INCA.

4.2 Sensitivity runs
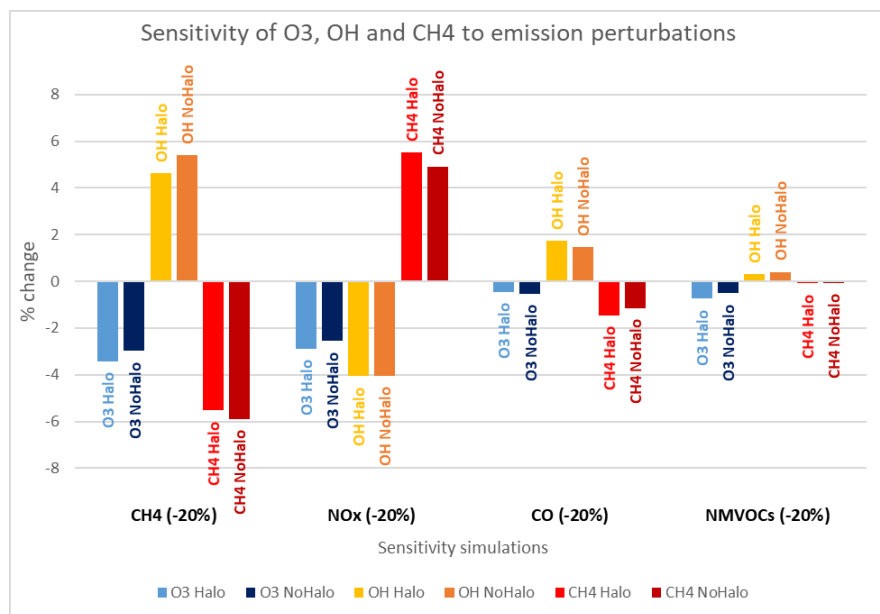
420   **Figure 8: Tropospheric relative changes (%) in ozone mass budget, OH concentration and methane lifetime for perturbation of NO$_x$, CO, NMVOCs emissions and CH$_4$ concentrations with and without halogen chemistry.**

In order to study the effect of halogen chemistry on the sensitivity of the tropospheric oxidative system, we explore, in Fig. 8, the relative changes (%) of ozone and OH when emissions of photooxidant precursors (NOx, CO and NMVOCs and of CH$_4$ concentrations are perturbed (-20%)). Our results show that the importance of sensitivities of ozone and OH to individual

425   photooxidant precursors emissions increase as follows in terms of importance: NMVOCs, CO, NO$_x$ and CH$_4$ (Fig. 8). It is also clear that the OH radical is more sensitive to perturbations in CH$_4$, NO$_x$ and CO than ozone. Notably, when accounting for halogens, ozone becomes more sensitive to changes in CH$_4$ and NO$_x$, and to a lesser extent to changes in NMVOCs. On the other hand, in the presence of halogen chemistry, the OH radical becomes more resilient in the presence of halogens to CH$_4$, NO$_x$ and NMVOCs perturbations. Traditionally, the chemical lifetime of CH$_4$ reflects the lifetime of CH$_4$ to removal by OH

430   in the troposphere and provides a useful proxy for global tropospheric oxidizing capacity (Wild et al., 2020). The simulations examined here show that the CH$_4$ lifetime with respect to OH remains a useful proxy for global tropospheric oxidizing capacity for all perturbations. However, in the presence of halogen chemistry, when NO$_x$ emissions are reduced, atomic chlorine, a secondary oxidant of methane, becomes more efficient and increase the sensitivity of CH$_4$ to NO$_x$ emission change. This exercise shows for the first time the influence of halogens on sensitivity of the tropospheric oxidative system to changes in the

435   emissions of photooxidant precursor (NO$_x$, CO and NMVOCs and of CH$_4$).

4.3 Impact on methane lifetime

The inclusion of tropospheric halogens affects the atmospheric concentrations of a large number of compounds in the model. A marked decrease in oxidants (O$_3$, OH, HO$_2$, H$_2$O$_2$) is then computed. This leads to an increase in the concentrations of CO (+8.5%) and some NMVOCs, including isoprene (+7.1%). The lifetime of methane with respect to chlorine and the OH radical

440   as well as the share of chlorine in the losses of methane in the literature are shown in Table 8. In the reference simulation, the tropospheric chemical lifetime of methane due to its consumption by OH is of 7.9 years. With the inclusion of halogen

chemistry, the OH concentration decreases, increasing this chemical lifetime of methane to 9.3 years. The chemical lifetime of methane linked to oxidation by Cl is 333 years, less than the 384 years suggested by Hossaini et al. (2016) but closer to IPCC AR5 estimates. This oxidation by Cl represents 2.7% of the total loss (close to the values reported in the literature and in Table 8). Thus, in LMDZ-INCA, accounting for both OH and the chlorinated radicals consumption, methane oxidation leads to a total chemical lifetime of CH_4 of 9.0 years.

Table 8: Methane lifetime with respect to chlorine and OH radical as well as the share of chlorine in methane losses in the literature.

	Lifetime relative to		Total chemical lifetime (years)	Method	Share of chlorine in methane loss (%)
	Chlorine (years)	OH radical (years)			
AR5 IPCC (2013)	200 ± 100	11.2 ± 1.3	9.25 ± 0.6	Multi evidence assessment	-
Hossaini et al. (2016)	384.4	10		TOMCAT model	2.5
Sherwen et al. (2016b)	-	8.28	8.16	GEOS-Chem model	2.0
Szopa et al. (2021)		9.7 ± 1.1	9.1 ± 0.9	Multi evidence assessment	
This work	-	7.9	7.9	**LMDZ-INCA model (NoHalo)**	-
	332.5	9.28	9.0	**LMDZ-INCA model (Halo)**	2.7

5 Conclusions

Global chemistry climate models allow to simulate the evolution of the atmospheric composition and are used for future projections in the framework of international model intercomparisons such as AerChemMIP. Most of these models do not account for halogen chemistry. We have implemented a simplified representation of the halogenated chemistry in the three-dimensional climate-chemistry model LMDZ-INCA to account for its effects on the tropospheric chemistry, notably ozone. First, the halogenated species, their sources and sinks, their reactions in the gas and heterogeneous phase and their physicochemical characteristics have been integrated into INCA. In order to simplify the integration of this chemistry, a chemical scheme already tested and evaluated in the CAM-Chem model has been used as a basis for our developments.

The representation of this chemistry has been shown to be sufficient in a first approach to simulate properly the impact of halogens on the photooxidizing system in the troposphere and particularly in the atmospheric boundary layer. The response of the tropospheric chemical system O_x, HO_x, NO_x, CH_4 and NMVOCs to incorporation of halogen chemistry has been quantified. On a global tropospheric scale, this chemistry induces decreases of the ozone burden by 22%, of OH by 8% and of NO_x by 33%. An increase in CO, NMVOC concentrations are simulated and the lifetime of methane increases by one year. These changes are consistent with those reported in the literature. Comparisons between simulations considering preindustrial and present-day emissions show that the sensitivity of the ozone burden to changes in emissions over the preindustrial era is ~ 20% lower in the presence of halogen chemistry (mainly because of the chemistry of iodine).

Sensitivity tests, consisting on reducing in turn the emissions of ozone precursors and methane concentrations, show for the first time that ozone becomes more sensitive to NO_x, CO and NMVOC perturbations in the presence of halogen chemistry.

Although still rarely represented in chemistry climate models, our model results confirm that the chemistry of tropospheric halogens (Cl, Br, I) plays a significant role in the global loss of tropospheric ozone. Since halogen chemistry affects substantially the ozone burden both in preindustrial and present-day chemical conditions and the ozone sensitivity to changes in anthropogenic emissions, international exercises examining the evolution of ozone between preindustrial, present, and future should consider to take into account halogen chemistry.

Data availability

The main model codes and the chemical scheme with halogenated compounds as well as the data outputs are publicly accessible through the doi: DOI WILL BE CREATED IF ACCEPTED

Author contributions

The implementation of the halogens chemical scheme has been done by CCaram, SS and AC. The design of the numerical simulations was conducted by CCaram, SS, AS-L and CCuevas. CCaram and SS prepared the Figures. CCaram, SS, SB, AS-L and CCuevas analyzed the results and drafted the paper.

Competing interests

The authors declare that they have no conflict of interest.

Acknowledgements

The authors are thankful to the NCAR Atmospheric Chemistry Division (ACD) for the distribution of the NCAR/ACD TUV: Tropospheric Ultraviolet & Visible Radiation Model (http://cprm.acom.ucar.edu/Models/TUV/Interactive_TUV/) and the availability of their quicktool.

Financial support

This research has been supported by the Agence Nationale de la Recherche (PALEOx project, grant no. ANR-16-CE31-0010). This work was granted access to the HPC resources of TGCC under the allocation A0090102212 made by GENCI (Grand Equipement National de Calcul Intensif). This study received funding from the European Research Council Executive Agency under the European Union's Horizon 2020 Research and Innovation Programme (Project ERC-2016- COG 726349 CLIMAHAL).

References

Abbatt, J. P. D., Thomas, J. L., Abrahamsson, K., Boxe, C., Granfors, A., Jones, A. E., King, M. D., Saiz-Lopez, A., Shepson, P. B., Sodeau, J., Toohey, D. W., Toubin, C., von Glasow, R., Wren, S. N., and Yang, X.: Halogen activation via interactions with environmental ice and snow in the polar lower troposphere and other regions, Atmos. Chem. Phys., 12, 6237–6271, https://doi.org/10.5194/acp-12-6237-2012, 2012.

Badia, A., Reeves, C. E., Baker, A. R., Saiz-Lopez, A., Volkamer, R., Koenig, T. K., Apel, E. C., Hornbrook, R. S., Carpenter, L. J., Andrews, S. J., Sherwen, T. and von Glasow, R.: Importance of reactive halogens in the tropical marine atmosphere: a regional modelling study using WRF-Chem, Atmos. Chem. Phys., 19(5), 3161–3189, doi:10.5194/acp-19-3161-2019, 2019.

Barker, J. R., Steiner, A. L. and Wallington, T. J.: Advances In Atmospheric Chemistry, Volume 1, World Scientific Publishing Company. [online] Available from: https://books.google.fr/books?id=3wGyDgAAQBAJ, 2016.

Bloss, W. J., Camredon, M., Lee, J. D., Heard, D. E., Plane, J. M. C., Saiz-Lopez, A., Bauguitte, S. J.-B., Salmon, R. A. and Jones, A. E.: Coupling of HO$_{x}$, NO$_{x}$ and halogen chemistry in the antarctic boundary layer, Atmos. Chem. Phys., 10(21), 10187–10209, doi:10.5194/acp-10-10187-2010, 2010.

Bottenheim, J. W., Barrie, L. A., Atlas, E., Heidt, L. E., Niki, H., Rasmussen, R. A. and Shepson, P. B.: Depletion of lower tropospheric ozone during Arctic spring: The Polar Sunrise Experiment 1988, J. Geophys. Res. Atmos., 95(D11), 18555–18568, doi:https://doi.org/10.1029/JD095iD11p18555, 1990.

Le Breton, M., Bannan, T. J., Shallcross, D. E., Khan, M. A., Evans, M. J., Lee, J., Lidster, R., Andrews, S., Carpenter, L. J.,

510 Schmidt, J., Jacob, D., Harris, N. R. P., Bauguitte, S., Gallagher, M., Bacak, A., Leather, K. E. and Percival, C. J.: Enhanced ozone loss by active inorganic bromine chemistry in the tropical troposphere, Atmos. Environ., 155, 21–28, doi:https://doi.org/10.1016/j.atmosenv.2017.02.003, 2017.

Carpenter, L., Reismann, S., Burkholder, J., Clerbaux, C., Hall, B., Hossaini, R., Laube, J. and Yvon-Lewis, S.: Ozone-Depleting Substances (ODSs) and other gases of interest to the Montreal Protocol, 2014.

515 Carpenter, L. J.: Iodine in the Marine Boundary Layer, Chem. Rev., 103(12), 4953–4962, doi:10.1021/cr0206465, 2003.

Carpenter, L. J., MacDonald, S. M., Shaw, M. D., Kumar, R., Saunders, R. W., Parthipan, R., Wilson, J. and Plane, J. M. C.: Atmospheric iodine levels influenced by sea surface emissions of inorganic iodine, Nat. Geosci., 6(2), 108–111, doi:10.1038/ngeo1687, 2013.

Chameides, W. L. and Davis, D. D.: Iodine: Its possible role in tropospheric photochemistry, J. Geophys. Res. Ocean., 85(C12),
520 7383–7398, doi:https://doi.org/10.1029/JC085iC12p07383, 1980.

Chen, D., Huey, L. G., Tanner, D. J., Salawitch, R. J., Anderson, D. C., Wales, P. A., Pan, L. L., Atlas, E. L., Hornbrook, R. S., Apel, E. C., Blake, N. J., Campos, T. L., Donets, V., Flocke, F. M., Hall, S. R., Hanisco, T. F., Hills, A. J., Honomichl, S. B., Jensen, J. B., Kaser, L., Montzka, D. D., Nicely, J. M., Reeves, J. M., Riemer, D. D., Schauffler, S. M., Ullmann, K., Weinheimer, A. J. and Wolfe, G. M.: Airborne measurements of BrO and the sum of HOBr and Br2 over the Tropical West
525 Pacific from 1 to 15 km during the CONvective TRansport of Active Species in the Tropics (CONTRAST) experiment, J. Geophys. Res. Atmos., 121(20), 12,512-560,578, doi:https://doi.org/10.1002/2016JD025561, 2016.

Cicerone, R. J.: Halogens in the atmosphere, Rev. Geophys., 19(1), 123–139, doi:https://doi.org/10.1029/RG019i001p00123, 1981.

Dix, B., Baidar, S., Bresch, J. F., Hall, S. R., Schmidt, K. S., Wang, S. and Volkamer, R.: Detection of iodine monoxide in the
530 tropical free troposphere, Proc. Natl. Acad. Sci. U. S. A., 110(6), 2035—2040, doi:10.1073/pnas.1212386110, 2013.

Dix, B., Koenig, T. K. and Volkamer, R.: Parameterization retrieval of trace gas volume mixing ratios from Airborne MAX-DOAS, Atmos. Meas. Tech., 9(11), 5655–5675, doi:10.5194/amt-9-5655-2016, 2016.

Dorf, M., Butz, A., Camy-Peyret, C., Chipperfield, M. P., Kritten, L. and Pfeilsticker, K.: Bromine in the tropical troposphere and stratosphere as derived from balloon-borne BrO observations, Atmos. Chem. Phys., 8(23), 7265–7271, doi:10.5194/acp-
535 8-7265-2008, 2008.

Fernandez, R. P., Salawitch, R. J., Kinnison, D. E., Lamarque, J.-F. and Saiz-Lopez, A.: Bromine partitioning in the tropical tropopause layer: implications for stratospheric injection, Atmos. Chem. Phys., 14(24), 13391–13410, doi:10.5194/acp-14-13391-2014, 2014a.

Fernandez, R. P., Ordóñez, C., Kinnison, D. E., Martín, J. C. G. and Lamarque, J.: Iodine chemistry in the troposphere and its
540 effect on ozone, , 13119–13143, doi:10.5194/acp-14-13119-2014, 2014b.

Folberth, G. A., Hauglustaine, D. A. and Lathi, J.: and Physics Interactive chemistry in the Laboratoire de Météorologie Dynamique general circulation model : model description and impact analysis of biogenic hydrocarbons on tropospheric chemistry, , 2273–2319, 2006.

Giorgi, F. and Chameides, W. L.: The rainout parameterization in a photochemical model, J. Geophys. Res. Atmos., 90(D5),
545 7872–7880, doi:10.1029/JD090iD05p07872, 1985.

von Glasow, R., Sander, R., Bott, A. and Crutzen, P. J.: Modeling halogen chemistry in the marine boundary layer 1. Cloud-free MBL, J. Geophys. Res. Atmos., 107(D17), ACH 9-1-ACH 9-16, doi:https://doi.org/10.1029/2001JD000942, 2002.

von Glasow, R., von Kuhlmann, R., Lawrence, M. G., Platt, U. and Crutzen, P. J.: Impact of reactive bromine chemistry in the troposphere, Atmos. Chem. Phys., 4(11/12), 2481–2497, doi:10.5194/acp-4-2481-2004, 2004.

550 Gómez Martín, J. C., Lewis, T. R., Blitz, M. A., Plane, J. M. C., Kumar, M., Francisco, J. S. and Saiz-Lopez, A.: A gas-to-particle conversion mechanism helps to explain atmospheric particle formation through clustering of iodine oxides, Nat. Commun., 11(1), 4521, doi:10.1038/s41467-020-18252-8, 2020.

Graedel, T. E. and Keene, W. C.: Tropospheric budget of reactive chlorine, Global Biogeochem. Cycles, 9(1), 47–77, doi:10.1029/94GB03103, 1995.

555 Hauglustaine, D. A., Hourdin, F., Jourdain, L., Filiberti, M., Walters, S., Lamarque, J. and Holland, E. A.: Interactive chemistry in the Laboratoire de Me ́te ́orologie Dynamique general circulation model : Description and background tropospheric chemistry evaluation, , 109, doi:10.1029/2003JD003957, 2004.

Hoesly, R. M., Smith, S. J., Feng, L., Klimont, Z., Janssens-Maenhout, G., Pitkanen, T., Seibert, J. J., Vu, L., Andres, R. J., Bolt, R. M., Bond, T. C., Dawidowski, L., Kholod, N., Kurokawa, J.-I., Li, M., Liu, L., Lu, Z., Moura, M. C. P., O'Rourke, P.

560 R. and Zhang, Q.: Historical (1750--2014) anthropogenic emissions of reactive gases and aerosols from the Community Emissions Data System (CEDS), Geosci. Model Dev., 11(1), 369–408, doi:10.5194/gmd-11-369-2018, 2018.

Holmes, C. D., Prather, M. J., Søvde, O. A. and Myhre, G.: Future methane, hydroxyl, and their uncertainties: key climate and emission parameters for future predictions, Atmos. Chem. Phys., 13(1), 285–302, doi:10.5194/acp-13-285-2013, 2013.

Hossaini, R., Chipperfield, M. P., Montzka, S. A., Rap, A., Dhomse, S. and Feng, W.: Efficiency of short-lived halogens at

565 influencing climate through depletion of stratospheric ozone, Nat. Geosci., 8(3), 186–190, doi:10.1038/ngeo2363, 2015.

Hossaini, R., Chipperfield, M. P., Saiz-Lopez, A., Fernandez, R., Monks, S., Feng, W., Brauer, P. and von Glasow, R.: A global model of tropospheric chlorine chemistry: Organic versus inorganic sources and impact on methane oxidation, J. Geophys. Res. Atmos., 121(23), 14,214-271,297, doi:https://doi.org/10.1002/2016JD025756, 2016.

Hu, L.: The Role of the Ocean in the Atmospheric Budgets of Methyl Bromide, Methyl Chloride and Methane, Dr. Diss. Texas

570 A&M Univ., 2012.

Iglesias-Suarez, F., Badia, A., Fernandez, R. P., Cuevas, C. A., Kinnison, D. E., Tilmes, S., Lamarque, J.-F., Long, M. C., Hossaini, R. and Saiz-Lopez, A.: Natural halogens buffer tropospheric ozone in a changing climate, Nat. Clim. Chang., 10(2), 147–154, doi:10.1038/s41558-019-0675-6, 2020.

Intergovernmental Panel on Climate Change, Ed.: Anthropogenic and natural radiative forcing, in Climate Change 2013 the

575 Physical Science Basis: Working Group I Contribution to the Fifth Assessment Report of the Intergovernmental Panel on Climate Change, vol. 9781107057, pp. 659–740, Cambridge University Press, Cambridge., 2013.

Keene, W. C., Stutz, J., Pszenny, A. A. P., Maben, J. R., Fischer, E. V, Smith, A. M., von Glasow, R., Pechtl, S., Sive, B. C. and Varner, R. K.: Inorganic chlorine and bromine in coastal New England air during summer, J. Geophys. Res. Atmos., 112(D10), doi:https://doi.org/10.1029/2006JD007689, 2007.

580 Leser, H., Hönninger, G. and Platt, U.: MAX-DOAS measurements of BrO and NO2 in the marine boundary layer, Geophys. Res. Lett., 30(10), doi:https://doi.org/10.1029/2002GL015811, 2003.

Lewis, T. R., Gómez Mart\'\in, J. C., Blitz, M. A., Cuevas, C. A., Plane, J. M. C. and Saiz-Lopez, A.: Determination of the absorption cross sections of higher-order iodine oxides at 355 and 532\,nm, Atmos. Chem. Phys., 20(18), 10865–10887, doi:10.5194/acp-20-10865-2020, 2020.

585 Lobert, J. M., Keene, W. C., Logan, J. A. and Yevich, R.: Global chlorine emissions from biomass burning: Reactive Chlorine Emissions Inventory, J. Geophys. Res. Atmos., 104(D7), 8373–8389, doi:https://doi.org/10.1029/1998JD100077, 1999.

Long, M. S., Keene, W. C., Easter, R. C., Sander, R., Liu, X., Kerkweg, A. and Erickson, D.: Sensitivity of tropospheric chemical composition to halogen-radical chemistry using a fully coupled size-resolved multiphase chemistry–global climate system: halogen distributions, aerosol composition, and sensitivity of climate-relevant gases, Atmos. Chem. Phys., 14(7),

590 3397–3425, doi:10.5194/acp-14-3397-2014, 2014.

Maasakkers, J. D., Jacob, D. J., Sulprizio, M. P., Scarpelli, T. R., Nesser, H., Sheng, J.-X., Zhang, Y., Hersher, M., Bloom, A. A., Bowman, K. W., Worden, J. R., Janssens-Maenhout, G. and Parker, R. J.: Global distribution of methane emissions, emission trends, and OH concentrations and trends inferred from an inversion of GOSAT satellite data for 2010--2015, Atmos. Chem. Phys., 19(11), 7859–7881, doi:10.5194/acp-19-7859-2019, 2019.

595 MacDonald, S. M., Gómez Martín, J. C., Chance, R., Warriner, S., Saiz-Lopez, A., Carpenter, L. J. and Plane, J. M. C.: A

a supprimé: Jacob, D. J.: Heterogeneous chemistry and tropospheric ozone, Atmos. Environ., 34(12), 2131–2159, doi:https://doi.org/10.1016/S1352-2310(99)00462-8, 2000.¶

laboratory characterisation of inorganic iodine emissions from the sea surface: dependence on oceanic variables and parameterisation for global modelling, Atmos. Chem. Phys., 14(11), 5841–5852, doi:10.5194/acp-14-5841-2014, 2014.

Mahajan, A. S., Plane, J. M. C., Oetjen, H., Mendes, L., Saunders, R. W., Saiz-Lopez, A., Jones, C. E., Carpenter, L. J. and McFiggans, G. B.: Measurement and modelling of tropospheric reactive halogen species over the tropical Atlantic Ocean, Atmos. Chem. Phys., 10(10), 4611–4624, doi:10.5194/acp-10-4611-2010, 2010.

Martin, M., Pöhler, D., Seitz, K., Sinreich, R. and Platt, U.: BrO measurements over the Eastern North-Atlantic, Atmos. Chem. Phys., 9(24), 9545–9554, doi:10.5194/acp-9-9545-2009, 2009.

McCulloch, A., Aucott, M. L., Benkovitz, C. M., Graedel, T. E., Kleiman, G., Midgley, P. M. and Li, Y.-F.: Global emissions of hydrogen chloride and chloromethane from coal combustion, incineration and industrial activities: Reactive Chlorine Emissions Inventory, J. Geophys. Res. Atmos., 104(D7), 8391–8403, doi:https://doi.org/10.1029/1999JD900025, 1999.

McFiggans, G., Plane, J. M. C., Allan, B. J., Carpenter, L. J., Coe, H. and O'Dowd, C.: A modeling study of iodine chemistry in the marine boundary layer, J. Geophys. Res. Atmos., 105(D11), 14371–14385, doi:10.1029/1999JD901187, 2000.

Molina, M. J. and Rowland, F. S.: Stratospheric sink for chlorofluoromethanes: chlorine atom-catalysed destruction of ozone, Nature, 249(5460), 810–812, doi:10.1038/249810a0, 1974.

Montzka S. A., S. Reimannander, Andreas Engel, Kirstin Kruger, O?Doherty Simon, William T. Sturges , Donald R. Blake , Marcel Dorf, Paul J. Fraser , Lucien Froidevaux , Kenneth Jucks, Karin Kreher, Michael J. Kurylo III, Abdelwahid Mellouki , Jo, D. P. V.: Ozone-Depleting Substances (ODSs) and Related Chemicals, Chapter 1 in Scientific Assessment of Ozone Depletion: 2010., 2011.

Naik, V., Voulgarakis, A., Fiore, A. M., Horowitz, L. W., Lamarque, J., Lin, M., Prather, M. J., Young, P. J., Plummer, D. A., Righi, M., Rumbold, S. T., Skeie, R., Shindell, D. T. and Stevenson, D. S.: Preindustrial to present-day changes in tropospheric hydroxyl radical and methane lifetime from the Atmospheric Chemistry and Climate Model Intercomparison Project (ACCMIP), , 5277–5298, doi:10.5194/acp-13-5277-2013, 2013.

O'Dowd, C. D., Jimenez, J. L., Bahreini, R., Flagan, R. C., Seinfeld, J. H., Hämeri, K., Pirjola, L., Kulmala, M., Jennings, S. G. and Hoffmann, T.: Marine aerosol formation from biogenic iodine emissions., Nature, 417(6889), 632–636, doi:10.1038/nature00775, 2002.

Oltmans, S. J. and Komhyr, W. D.: Surface ozone distributions and variations from 1973–1984: Measurements at the NOAA Geophysical Monitoring for Climatic Change Baseline Observatories, J. Geophys. Res. Atmos., 91(D4), 5229–5236, doi:https://doi.org/10.1029/JD091iD04p05229, 1986.

Ordóñez, C., Lamarque, J.-F., Tilmes, S., Kinnison, D. E., Atlas, E. L., Blake, D. R., Sousa Santos, G., Brasseur, G. and Saiz-Lopez, A.: Bromine and iodine chemistry in a global chemistry-climate model: description and evaluation of very short-lived oceanic sources, Atmos. Chem. Phys., 12(3), 1423–1447, doi:10.5194/acp-12-1423-2012, 2012.

Ordóñez, C., Lamarque, J., Tilmes, S., Kinnison, D. E., Atlas, E. L., Blake, D. R., Santos, G. S. and Brasseur, G.: Bromine and iodine chemistry in a global chemistry- climate model : Description and evaluation of very short-lived oceanic sources, Atmos. Chem. Phys., 12, 1423–1447, https://doi.org/10.5194/acp-12-1423-2012, 2012.

Parrella, J. P., Jacob, D. J., Liang, Q., Zhang, Y., Mickley, L. J., Miller, B., Evans, M. J., Yang, X., Pyle, J. A., Theys, N. and Van Roozendael, M.: Tropospheric bromine chemistry: implications for present and pre-industrial ozone and mercury, Atmos. Chem. Phys., 12(15), 6723–6740, doi:10.5194/acp-12-6723-2012, 2012b.

Platt, U. and Hönninger, G.: The role of halogen species in the troposphere., Chemosphere, 52(2), 325–338, doi:10.1016/S0045-6535(03)00216-9, 2003.

Prados-Roman, C., Butz, A., Deutschmann, T., Dorf, M., Kritten, L., Minikin, A., Platt, U., Schlager, H., Sihler, H., Theys, N., Van Roozendael, M., Wagner, T. and Pfeilsticker, K.: Airborne DOAS limb measurements of tropospheric trace gas profiles: case studies on the profile retrieval of O$_{4}$ and BrO, Atmos. Meas. Tech., 4(6), 1241–1260, doi:10.5194/amt-4-1241-2011, 2011.

---

a supprimé: 1

a supprimé: –15, n.d.

a supprimé: Parrella, J. P., Jacob, D. J., Liang, Q., Zhang, Y., Mickley, L. J., Miller, B., Evans, M. J., Yang, X. and Pyle, J. A.: and Physics Tropospheric bromine chemistry : implications for present and pre-industrial ozone and mercury, , 6723–6740, doi:10.5194/acp-12-6723-2012, 2012a.¶

Prados-Roman, C., Cuevas, C. A., Fernandez, R. P., Kinnison, D. E., Lamarque, J.-F. and Saiz-Lopez, A.: A negative feedback
between anthropogenic ozone pollution and enhanced ocean emissions of iodine, Atmos. Chem. Phys., 15(4), 2215–2224,
doi:10.5194/acp-15-2215-2015, 2015a.

Prados-Roman, C., Cuevas, C. A., Hay, T., Fernandez, R. P., Mahajan, A. S., Royer, S.-J., Galí, M., Simó, R., Dachs, J.,
Großmann, K., Kinnison, D. E., Lamarque, J.-F. and Saiz-Lopez, A.: Iodine oxide in the global marine boundary layer, Atmos.
Chem. Phys., 15(2), 583–593, doi:10.5194/acp-15-583-2015, 2015b.

Prather, M. J., Holmes, C. D. and Hsu, J.: Reactive greenhouse gas scenarios: Systematic exploration of uncertainties and the
role of atmospheric chemistry, Geophys. Res. Lett., 39(9), doi:10.1029/2012GL051440, 2012.

Puentedura, O., Gil, M., Saiz-Lopez, A., Hay, T., Navarro-Comas, M., Gómez-Pelaez, A., Cuevas, E., Iglesias, J. and Gomez,
L.: Iodine monoxide in the north subtropical free troposphere, Atmos. Chem. Phys., 12(11), 4909–4921, doi:10.5194/acp-12-
4909-2012, 2012.

Read, K. A., Mahajan, A. S., Carpenter, L. J., Evans, M. J., Faria, B. V. E., Heard, D. E., Hopkins, J. R., Lee, J. D., Moller, S.
J., Lewis, A. C., Mendes, L., Mcquaid, J. B., Oetjen, H., Saiz-lopez, A., Pilling, M. J. and Plane, J. M. C.: Extensive halogen-
mediated ozone destruction over the tropical Atlantic Ocean, , 453(June), 1232–1236, doi:10.1038/nature07035, 2008.

Sadourny, R. and Laval, K.: New perspectives in climate modelling, 1984.

Saiz-Lopez A., Plane, J. M. C.: Novel iodine chemistry in the marine boundary layer, Geophysical Research Letters,
https://doi.org/10.1029/2003GL019215, 2004.

Saiz-lopez, A. and Von Glasow, R.: Chem Soc Rev, , 6448–6472, doi:10.1039/c2cs35208g, 2012.

Saiz-Lopez, A., Plane, J. M. C., Baker, A. R., Carpenter, L. J., von Glasow, R., Gómez Martín, J. C., McFiggans, G. and
Saunders, R. W.: Atmospheric Chemistry of Iodine, Chem. Rev., 112(3), 1773–1804, doi:10.1021/cr200029u, 2012a.

Saiz-Lopez, A., Lamarque, J.-F., Kinnison, D. E., Tilmes, S., Ordóñez, C., Orlando, J. J., Conley, A. J., Plane, J. M. C.,
Mahajan, A. S., Sousa Santos, G., Atlas, E. L., Blake, D. R., Sander, S. P., Schauffler, S., Thompson, A. M. and Brasseur, G.:
Estimating the climate significance of halogen-driven ozone loss in the tropical marine troposphere, Atmos. Chem. Phys.,
12(9), 3939–3949, doi:10.5194/acp-12-3939-2012, 2012b.

Saiz-Lopez, A., Fernandez, R. P., Ordóñez, C., Kinnison, D. E., Gómez Martín, J. C., Lamarque, J.-F. and Tilmes, S.: Iodine
chemistry in the troposphere and its effect on ozone, Atmos. Chem. Phys., 14(23), 13119–13143, doi:10.5194/acp-14-13119-
2014, 2014.

Saiz-Lopez, A., Baidar, S., Cuevas, C. A., Koenig, T. K., Fernandez, R. P., Dix, B., Kinnison, D. E., Lamarque, J.-F.,
Rodriguez-Lloveras, X., Campos, T. L. and Volkamer, R.: Injection of iodine to the stratosphere, Geophys. Res. Lett., 42(16),
6852–6859, doi:https://doi.org/10.1002/2015GL064796, 2015.

Saltzman, E. S., Aydin, M., De Bruyn, W. J., King, D. B. and Yvon-Lewis, S. A.: Methyl bromide in preindustrial air:
Measurements from an Antarctic ice core, J. Geophys. Res. Atmos., 109(D5), doi:https://doi.org/10.1029/2003JD004157,
2004.

Sander, S., Friedl, R., Golden, D., Kurylo, M., Huie, R., Orkin, V., Moortgat, G., Ravishankara, A. R., Kolb, C., Molina, M.
and Finlayson-Pitts, B.: Chemical Kinetics and Photochemical Data for Use in Atmosheric Studies; JPL Publication 02-25,
2003.

Sander, SP; Abbatt, JPD; Barker, JR; Burkholder, JB; Friedl, RR; Golden, DM; Huie, RE; Kolb, CE; Kurylo, MJ; Moortgat,
GK; Orkin, VL; Wine, PH, Chemical kinetics and photochemical data for use in atmospheric studies: Evaluation number 17 ,
Technical Report 2011 , JPL Publication 10-6 , http://jpldataeval.jpl.nasa.gov/pdf/JPL%2010-6%2015June2011.pdf

Schmidt, J. A., Jacob, D. J., Horowitz, H. M., Hu, L., Sherwen, T., Evans, M. J., Liang, Q., Suleiman, R. M., Oram, D. E.,
Breton, M. Le, Percival, C. J., Wang, S., Dix, B. and Volkamer, R.: Modeling the observed tropospheric BrO background :
Importance of multiphase chemistry and implications for ozone, OH, and mercury, 819–835, doi:10.1002/2015JD024229.
2016.

Sherwen, T., Schmidt, J. A., Evans, M. J., Carpenter, L. J., Großmann, K., Volkamer, R., Saiz-lopez, A., Prados-roman, C., Mahajan, A. S. and Ordóñez, C.: Global impacts of tropospheric halogens (Cl , Br , I) on oxidants and composition in GEOS-

700   Chem, 12239–12271, doi:10.5194/acp-16-12239-2016, 2016a.

Sherwen, T., Evans, M. J., Carpenter, L. J., Andrews, S. J., Lidster, R. T., Dix, B., Koenig, T. K. and Sinreich, R.: Iodine ' s impact on tropospheric oxidants : a global model study in GEOS-Chem, , 1161–1186, doi:10.5194/acp-16-1161-2016, 2016b.

Sherwen, T., Evans, M. J., Carpenter, L. J., Schmidt, J. A. and Mickley, L. J.: Halogen chemistry reduces tropospheric O 3 radiative forcing, , 1557–1569, doi:10.5194/acp-17-1557-2017, 2017.

705   Simpson, W. R., Brown, S. S., Glasow, R. Von, Saiz-lopez, A. and Thornton, J. A.: Tropospheric Halogen Chemistry : Sources , Cycling , and Impacts, , doi:10.1021/cr5006638, 2015.

Stolarski, R. S. and Cicerone, R. J.: Stratospheric Chlorine: a Possible Sink for Ozone, Can. J. Chem., 52(8), 1610–1615, doi:10.1139/v74-233, 1974.

Stone, D., Whalley, L. K. and Heard, D. E.: Tropospheric OH and HO2 radicals: field measurements and model comparisons,

710   Chem. Soc. Rev., 41(19), 6348–6404, doi:10.1039/C2CS35140D, 2012.

Szopa, S., V. Naik, B. Adhikary, P. Artaxo, T. Berntsen, W.D. Collins, S. Fuzzi, L. Gallardo, A. Kiendler Scharr, Z. and Klimont, H. Liao, N. Unger, P. Z.: Short-Lived Climate Forcers, in Climate Change 2021: The Physical Science Basis. Contribution of Working Group I to the Sixth Assessment Report of the Intergovernmental Panel on Climate Change, Cambridge University Press., 2021.

715   Szopa, S., Balkanski, Y., Schulz, M., Bekki, S., Cugnet, D., Fortems-Cheiney, A., Turquety, S., Cozic, A., Déandreis, C., Hauglustaine, D., Idelkadi, A., Lathière, J., Lefevre, F., Marchand, M., Vuolo, R., Yan, N. and Dufresne, J.-L.: Aerosol and ozone changes as forcing for climate evolution between 1850 and 2100, Clim. Dyn., 40(9), 2223–2250, doi:10.1007/s00382-012-1408-y, 2013.

Volkamer, R., Baidar, S., Campos, T. L., Coburn, S., DiGangi, J. P., Dix, B., Eloranta, E. W., Koenig, T. K., Morley, B.,

720   Ortega, I., Pierce, B. R., Reeves, M., Sinreich, R., Wang, S., Zondlo, M. A. and Romashkin, P. A.: Aircraft measurements of BrO, IO, glyoxal, NO_2, H_2O, O_2–O_2 and aerosol extinction profiles in the tropics: comparison with aircraft-/ship-based in situ and lidar measurements, Atmos. Meas. Tech., 8(5), 2121–2148, doi:10.5194/amt-8-2121-2015, 2015.

Voulgarakis, A., Naik, V., Lamarque, J.-F., Shindell, D. T., Young, P. J., Prather, M. J., Wild, O., Field, R. D., Bergmann, D.,

725   Cameron-Smith, P., Cionni, I., Collins, W. J., Dalsøren, S. B., Doherty, R. M., Eyring, V., Faluvegi, G., Folberth, G. A., Horowitz, L. W., Josse, B., MacKenzie, I. A., Nagashima, T., Plummer, D. A., Righi, M., Rumbold, S. T., Stevenson, D. S., Strode, S. A., Sudo, K., Szopa, S. and Zeng, G.: Analysis of present day and future OH and methane lifetime in the ACCMIP simulations, Atmos. Chem. Phys., 13(5), 2563–2587, doi:10.5194/acp-13-2563-2013, 2013.

Wang, S., Schmidt, J. A., Baidar, S., Coburn, S., Dix, B., Koenig, T. K., Apel, E., Bowdalo, D., Campos, T. L., Eloranta, E.,

730   Evans, M. J., DiGangi, J. P., Zondlo, M. A., Gao, R.-S., Haggerty, J. A., Hall, S. R., Hornbrook, R. S., Jacob, D., Morley, B., Pierce, B., Reeves, M., Romashkin, P., ter Schure, A. and Volkamer, R.: Active and widespread halogen chemistry in the tropical and subtropical free troposphere, Proc. Natl. Acad. Sci., 112(30), 9281 LP – 9286, doi:10.1073/pnas.1505142112, 2015.

Wang, X., Jacob, D. J., Eastham, S. D., Sulprizio, M. P., Zhu, L., Chen, Q., Alexander, B., Sherwen, T., Evans, M. J., Lee, B.

735   H., Haskins, J. D., Lopez-Hilfiker, F. D., Thornton, J. A., Huey, G. L. and Liao, H.: The role of chlorine in global tropospheric chemistry, Atmos. Chem. Phys., 19(6), 3981–4003, doi:10.5194/acp-19-3981-2019, 2019.

Wang, X., Jacob, D. J., Downs, W., Zhai, S., Zhu, L., Shah, V., Holmes, C. D., Sherwen, T., Alexander, B., Evans, M. J., Eastham, S. D., Neuman, J. A., Veres, P., Koenig, T. K., Volkamer, R., Huey, L. G., Bannan, T. J., Percival, C. J., Lee, B. H. and Thornton, J. A.: Global tropospheric halogen (Cl, Br, I) chemistry and its impact on oxidants, Atmos. Chem. Phys.

740   Discuss., 2021, 1–34, doi:10.5194/acp-2021-441, 2021.

Wang, Y. and Jacob, D. J.: Anthropogenic forcing on tropospheric ozone and OH since preindustrial times, J. Geophys. Res. Atmos., 103(D23), 31123–31135, doi:10.1029/1998JD100004, 1998.

Wesely, M. L.: Parameterization of surface resistances to gaseous dry deposition in regional-scale numerical models, Atmos. Environ., 23(6), 1293–1304, doi:https://doi.org/10.1016/0004-6981(89)90153-4, 1989.

745   Wild, O. and Palmer, P.: How sensitive is tropospheric oxidation to anthropogenic emissions, Geophys. Res. Lett., 35, 2008.

Wild, O., Voulgarakis, A., O'Connor, F., Lamarque, J.-F., Ryan, E. M. and Lee, L.: Global sensitivity analysis of chemistry--climate model budgets of tropospheric ozone and OH: exploring model diversity, Atmos. Chem. Phys., 20(7), 4047–4058, doi:10.5194/acp-20-4047-2020, 2020.

Worton, D. R., Sturges, W. T., Schwander, J., Mulvaney, R., Barnola, J.-M. and Chappellaz, J.: 20th century trends and budget
750   implications of chloroform and related tri-and dihalomethanes inferred from firn air, Atmos. Chem. Phys., 6(10), 2847–2863, doi:10.5194/acp-6-2847-2006, 2006.

Yang, X., Cox, R. A., Warwick, N. J., Pyle, J. A., Carver, G. D., O'Connor, F. M. and Savage, N. H.: Tropospheric bromine chemistry and its impacts on ozone: A model study, J. Geophys. Res. Atmos., 110(D23), doi:https://doi.org/10.1029/2005JD006244, 2005.

755   Young, P. J., Archibald, A. T., Bowman, K. W., Lamarque, J.-F., Naik, V., Stevenson, D. S., Tilmes, S., Voulgarakis, A., Wild, O., Bergmann, D., Cameron-Smith, P., Cionni, I., Collins, W. J., Dalsøren, S. B., Doherty, R. M., Eyring, V., Faluvegi, G., Horowitz, L. W., Josse, B., Lee, Y. H., MacKenzie, I. A., Nagashima, T., Plummer, D. A., Righi, M., Rumbold, S. T., Skeie, R. B., Shindell, D. T., Strode, S. A., Sudo, K., Szopa, S. and Zeng, G.: Pre-industrial to end 21st century projections of tropospheric ozone from the Atmospheric Chemistry and Climate Model Intercomparison Project (ACCMIP), Atmos. Chem.
760   Phys., 13(4), 2063–2090, doi:10.5194/acp-13-2063-2013, 2013.

Zhu, L., Jacob, D. J., Eastham, S. D., Sulprizio, M. P., Wang, X., Sherwen, T., Evans, M. J., Chen, Q., Alexander, B., Koenig, T. K., Volkamer, R., Huey, L. G., Le Breton, M., Bannan, T. J. and Percival, C. J.: Effect of sea salt aerosol on tropospheric bromine chemistry, Atmos. Chem. Phys., 19(9), 6497–6507, doi:10.5194/acp-19-6497-2019, 2019.

Copernicus Publications
The Innovative Open Access Publisher

765